SUPPORTING INFORMATION

Synthesis and biological evaluation of some bicyclic [2- (2, 4-dimethylphenylthio) phenyl] aniline and its amide derivatives as potential antitubercular agents

YOGESH PATIL,[a] RAMESH SHINGARE,[a] SHAKTI CHAKRABORTY,[b] RACHANA BORKUTE,[b] DHIMAN SARKAR[b] and BALAJI MADJE[a,*]

[a]Department of Chemistry, Vasantrao Naik Mahavidhyalaya, Aurangabad, Maharashtra, 431 003, India

[b]Combi Chem Bio Resource Centre, National Chemical Laboratory, Pune, Maharashtra, 411 008, India

Email. drmadjebr@gmail.com

Content of the supplementary Information:

1. Experimental details

All the chemicals such as sodium salt XTT and MTT, DMSO, ampicillin and rifampicin were purchased from Sigma-Aldrich, USA. Dubos medium was purchased from DIFCO, USA. Synthesized compounds were dissolved in DMSO and it was used as stock solution (10mg/ml) for further biological testing.

1.1 Cultivation of mycobacteria

Microbial strains such as *Mycobacterium tuberculosis* H37Ra (ATCC 25177) was obtained from AstraZeneca, India. The stock culture was maintained at -80^{o}C and subcultured once in a liquid medium before inoculation into an experimental culture. Cultures were grown in Dubos media (enrichment media). For antimycobacterial assay, *M. pheli* medium (minimal essential medium) was used. It contains 0.5 g KH_2PO_4, 0.25 g trisodium citrate, 60 mg MgSO4, 0.5 g aspargine and 2 ml glycerol in distilled water (100 ml) followed by pH adjustment to 6.6. All bacterial stock cultures were first grown in Dubos media at 37 ^{o}C at 150 RPM. It takes at least 8-10 days for OD 1 at 620 nm. The antimycobacterial assay was performed in 96-well plates for active as well as dormant stages.

1.2 Anti-tubercular activity

The antitubercular activity for each synthesized compound was determined by measuring inhibition of growth against a virulent strain of *M.tuberculosis* H37Ra (MTB, Dormant stage) (ATCC 25177) in liquid medium using an established XTT Reduction Menadione assay (XRMA) method. The optical density was read on a micro plate reader (Spectramax plus384 plate reader, Molecular Devices Inc) at 470 nm filter against a blank prepared from cell-free wells. Absorbance given by cells treated with the vehicle alone was taken as 100% cell growth. Initially primary screening was done at 30, 10 and 3 µg/ml. Compounds showing

90% inhibition of bacilli at 30 µg/ml which were selected for further dose response curve. MIC and IC_{50} values of selected compound were calculated from their dose response curves (30 to 0.23 µg/ mL) by using Origin 6 software. Percent inhibition was calculated by using following formula: % Inhibition = [(absorbance of Control − absorbance of Test)/(absorbance of Control – absorbance of Blank)] × 100, where control is the medium with bacillialong with vehicle and blank is cell free medium. The drug in clinical use, rifampicin was used as reference.

Table S1. *In vitro* antitubercular activity of compounds against Active and Dormant strain of MDR *MTB* H37Ra.

Compound	***M. Tuberculosis* H37Ra (ACTIVE)**		***M. Tuberculosis* H37Ra (DORMANT)**	
	IC_{50} (µg/mL)	MIC90 (µg/mL)	IC_{50} (µg/mL)	MIC90 (µg/mL)
6a	2.22	19.3	0.07	7.46
6b	6.32	>30	0.95	18.88
6c	>30	>30	>30	>30
6d	6.51	>30	1.93	25.58
6e	>30	>30	>30	>30
6f	>30	>30	>30	>30
6g	24.64	>30	4.37	25.3
6h	25.3	>30	>30	>30
6i	>30	>30	>30	>30
6j	0.05	17.48	0.15	4.54
6k	>30	>30	>30	>30
6l	1.64	>30	0.66	21.02

6m	0.75	19.76	0.36	6.77
6n	<0.01	9.34	<0.01	0.37
6o	>30	>30	>30	>30
Rifampicin	0.020	0.53	0.0019	0.80

Table S2. *Ex-vivo* antitubercular activity of compounds against strain of Active and Dormant *MTB* H37Ra.

Compound	***M. Tuberculosis* H37Ra (ACTIVE)**		***M. Tuberculosis* H37Ra (DORMANT)**	
	IC_{50} (µg/mL)	MIC90 (µg/mL)	IC_{50} (µg/mL)	MIC90 (µg/mL)
6a	1.24	23.28	0.086	7.33
6j	0.46	24.9	0.17	5.78
6n	<0.01	6.04	<0.01	2.72
Rifampicin	0.020	0.53	0.0019	0.80

1.3 Antibacterial activity

Bacterial strains *E. coli* (NCIM 2688), *P. aeruginosa* (NCIM 2036) as gram-negative and *B. subtilus* (NCIM 2079), *S. aureus* (NCIM 2010) as gram-positive were obtained from NCIM (NCL, Pune) and were grown in Luria Burtony medium from Himedia, India. Once the culture reaches 1 $O.D_{620}$, it was used for anti-bacterial assay. Briefly, 0.1 OD_{620} bacterial culture was treated with synthesized compound at 3µg/mL concentration and incubated for 8 hrs at 37 C. Ampicillin served as positive control for antibacterial activity. The *in vitro*

preliminary screening values (% inhibition) against microorganisms tested are summarized in **Tables S3**.

Table S3. Primary anti-bacterial activity of compounds against strain of Bacteria at single concentration.

	P. aeruginosa	***S. aureus***	***B. subtilis***	***E.coli***
6a	-1.14	-3.31	44.35	10.92
6b	-8.01	-6.21	7.40	11.33
6c	-6.41	-9.31	-8.26	14.12
6d	-5.30	-9.53	-6.38	14.71
6e	-7.37	-4.65	-6.82	13.64
6f	-8.92	-6.06	-6.97	25.48
6g	-9.02	-1.57	-8.29	27.32
6h	-7.94	-9.01	-6.95	-4.58
6i	-8.36	-7.72	-7.30	2.88
6j	-6.59	-2.35	23.10	1.86
6k	-3.00	-7.85	-7.32	-8.92
6l	-9.01	-2.24	-4.85	-4.73
6m	-12.61	1.87	23.75	5.01
6n	-8.09	-2.53	48.44	-3.88
6o	-7.98	-3.67	10.75	12.16

The % Inhibition in the presence of test material (at 3µg/ml concentration) is calculated by following formula.

% inhibition = (Average of Control-Average of Compound)/ (Average of Control-Average of Blank) X 100

Where control is culture medium with cells and DMSO and blank is culture medium without cells.

1.4 Cytotoxicity assay

Three human cancer cell lines, HeLa (human cervical cancer), MCF-7 (human mammary epithelial), THP-1 (human monocytic leukemia) cell line were used to check the cytotoxicity of compounds. The cell lines were obtained from the National Centre for Cell Science (NCCS), Pune and maintained in T25 flasks with 10 % (v/v) fetal bovine serum (FBS) containing Dulbecco's Modified Eagle Medium (DMEM). Cell line containing T25 flasks were maintained at 37 ºC under 5% CO_2 and 95% air in a humidified atmosphere. Medium were replaced twice a week. All the compounds were tested for their cytotoxicity against the mentioned cell line by using modified MTT assay as described previously (*Singh R et al., 2015*). Briefly, HeLa, MCF-7cells were seeded at the density of 1×10^4 cells/ml in a 96 well plate. The plates were incubated overnight into CO_2 incubator (37 ºC under 5% CO_2 and 95% air in a humidified atmosphere) to adhere the cells. Next day, cells were treated with different concentration of test compounds (100-0µg/ml) and incubated for additional 48h. Post incubation, cell medium was replaced with MTT (0.5mg/ml)-PBS medium and incubated for 2-4h to form the reduced MTT or Formazan crystals. This reduced MTT or Formazan crystals were solubilized by addition of acidified isopropanol. The optical density was read on a micro plate reader (Spectramax plus384 plate reader, Molecular Devices Inc) at 570nm filter against a blank prepared from cell-free wells. Absorbance given by cells treated with

the vehicle alone was taken as 100% cell growth. IC_{50} and MIC values were calculated by plotting the graphs, by using Origin Pro software. The viability and growth in the presence of test material is calculated by using the following formula: Percent cytotoxicity = [(average absorbance of control − absorbance of compound)/(absorbance of control – absorbance of blank)] × 100, where control is the culture medium with cells and DMSO and blank is the culture medium without cells.

Table S4. Growth inhibition concentration on three human cell lines.

Compound	THP-1		HeLa		MCF-7	
	GI_{50} (µg/ml)	**GI_{90} (µg/ml)**	**GI_{50} (µg/ml)**	**GI_{90} (µg/ml)**	**GI_{50} (µg/ml)**	**GI_{90} (µg/ml)**
6a	78.84	>100	20.33	36.83	2.247	>100
6j	>100	>100	46.77	>100	2.345	>100
6n	>100	>100	61.78	>100	1.905	>100
Rifampicin	>100	>100	>100	>100	>100	>100

1.5 Selectivity Index

The selectivity index (SI) was calculated by dividing the 50% growth inhibition concentration (GI_{50}) for cell lines (HeLa, MCF-7 and THP-1) by the MIC for *in vitro* activity against active/dormant MTB and MDR-MTB (*Kuete V., 2010*)

Table S5. Selectivity index of selected active analogues against *Mycobacterium tuberculosis* H37Ra In vitro and Ex vivo model.

Comp ID	THP-1		HeLa		MCF-7	
	In vitro	*Ex vivo*	*In vitro*	*Ex vivo*	*In vitro*	*Ex vivo*
6a	10.56836	10.7558	2.72	2.77	0.30	0.30
6j	22.02643	17.30104	10.30	8.09	0.51	0.40
6n	270.2703	36.76471	166.97	22.71	5.14	0.70

1.6 Docking studies

In an effort to rationalize the observed biological results and to gain an insight into binding mode and the thermos dynamic interactions that govern the binding of the most active bicyclic [2-(2,4-dimethylphenylthio)phenyl] aniline derivative **6a**, **6j**, and **6n** with the target enzyme, mycobacterial enoyl reductase (InhA) molecular docking study was performed.. The docking score of most active compounds **6a**, **6j**, and **6n** was found to be -9.668, -9.964, and -10.027 respectively which were comparable with their vitro antitubercular activity of these compounds. To make the discussion brief here we have discussed only the docking studies of most active compounds **6j** and **6n**. The interactions of **6j** and **6n** with the active site of mycobacterial InhA is shown in **Figure S1** and **Figure S2**.

The lowest energy docking pose of **6j** and **6n** revealed the presence of highly hydrophobic π-π stacking interactions between benzamine ring with the both Tyr158 and Phe149 and with Phe149 amino acid residues respectively which leads to little less docking score of **6j** as observed in **Figure S1** and **Figure S2**. Further, hydrogen bonding interactions were observed between –C=O of the acetyl group of the compound **6n** with Tyr158 with the distance of 2.29A°, while –C=O of the acetyl group of compound **6j** showed hydrogen bonding interactions with Thr196 with the distance of 2.16A°.Also, dimethylphenylthio ring

of compound **6j** and **6n** fits into the hydrophobic pocket of the active site of InhA which was formed by the hydrophobic side chains of amino acid residues Gly104, Met155, Pro156, Ala157, Leu207, Ala211, Ile215, Leu218, and Met103. These, firm hydrogen bonding and π-π stacking interactions help in the orientation of these ligands within the active site which increases the steric and electrostatic interactions of ligands with the amino acid residues present within the active site of mycobacterial InhA.

The per residue interaction analysis explains the differences which were observed in binding affinity of bicyclic [2-(2,4-dimethylphenylthio)phenyl] aniline derivatives with the active site of InhA. (Data represented in **Table S6**)

Table S6. Quantitative estimation of the per-residue interactions analysis of bicyclic [2-(2,4-dimethylphenylthio)phenyl] aniline derivatives with the active site of *Mycobacterium tuberculosis* enoyl-acyl carrier protein reductase (InhA).

Compound	**Docking score**	**Per-residue interaction energy analysis**		**Hydrogen Bonding (A°)**
		Van der Waals energy (kcal/mol)	**Electrostatic energy (kcal/mol)**	
6j	-9.964	Leu218 (-2.183), Ile215 (-2.802), Ile202 (-1.245), Met199 (-3.684), Ala198 (-0.803), Thr196 (-0.970), Met161 (-2.596), Tyr158 (-6.352), Ala157 (-2.117), Pro156 (-1.395), Met155 (-1.902), Phe149 (-3.403), Met103 (-3.494), Met98 (-	Leu218 (-2.540), Ile215 (-3.086), Ile202 (-2.296), Met199 (-4.308), Ala198 (-3.394), Thr196 (-3.867), Met161 (-4.384), Tyr158 (-9.445), Ala157 (-1.988), Pro156 (-1.242), Met155 (-1.321), Phe149 (-3.118), Met103 (-	Thr196 (2.16 Å)

		1.249), and Phe97 (-1.657)	3.736), Met98 (-0.932), and Phe97 (-1.628)	
6n	-10.027	Leu218 (-1.073), Ile215 (-3.080), Leu207 (-1.073), Ile202 (-2.482), Met199 (-4.297), Ala198 (-1.707), Thr196 (-0.965), Met161 (-1.876), Tyr158 (-6.696), Ala157 (-2.124), Pro156 (-1.457), Met155 (-2.160), Phe149 (-3.232), Met103 (-4.240), Met98 (-1.607), and Phe97 (-2.099)	Leu218 (-1.002), Ile215 (-3.164), Leu207 (-1.059), Ile202 (-2.344), Met199 (-4.949), Ala198 (-2.515), Thr196 (-4.047), Met161 (-1.900), Tyr158 (-7.337), Ala157 (-2.324), Pro156 (-2.141), Met155 (-2.043), Phe149 (-3.627), Met103 (-3.821), Met98 (-1.585), and Phe97 (-2.205)	Tyr158 (2.29 Å)

Docking studies were validated by extracting the native ligand 641 from the active site of and docking it again with the active site of InhA. The RMSD value obtained of the redocked conformation was less than 1A° than the original conformation of 4TZK which validates the dependability and duplicability of our docking studies.

A significant correlation was observed between the binding scores of the docked ligands and MIC values which confirm that bicyclic [2-(2,4-dimethylphenylthio)phenyl] aniline and its derivatives have the same kind of binding as that of native ligand 641 which further validates our docking studies. Hence, the probable mechanism of action for

antitubercular activity of bicyclic [2-(2,4-dimethylphenylthio)phenyl] aniline and its derivatives might be through inhibition of active site of InhA which further needs to be validated by in vitro studies.

Figure S1. 3D and 2D view of binding of compound **6j** with the active site of mycobacterial InhA

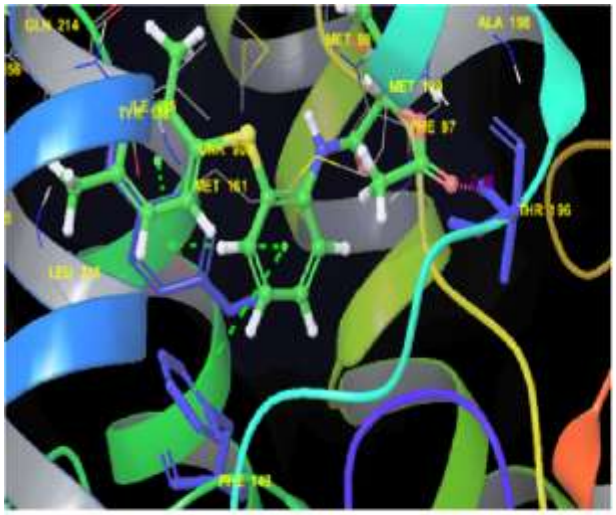

3D view of binding of compound **6j**

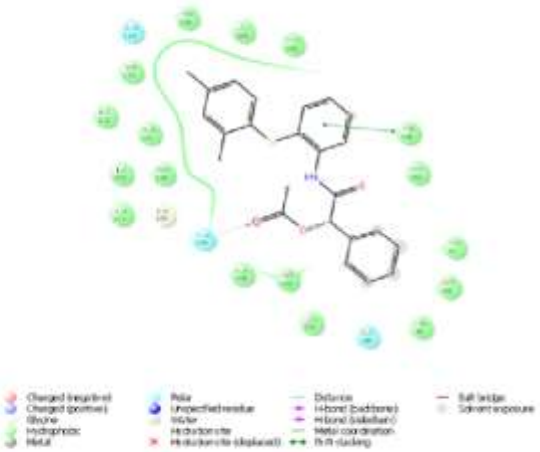

2D view of binding of compound **6j**

Figure S2. 3D and 2D view of binding of compound **6n** with the active site of mycobacterial InhA

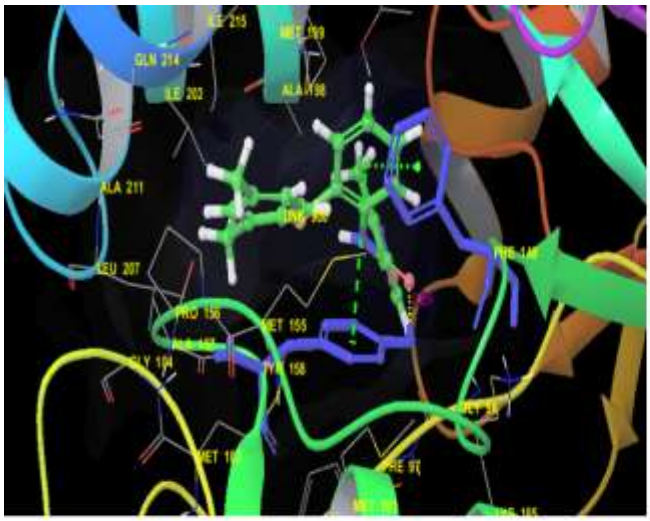

3D view of binding of compound **6n**

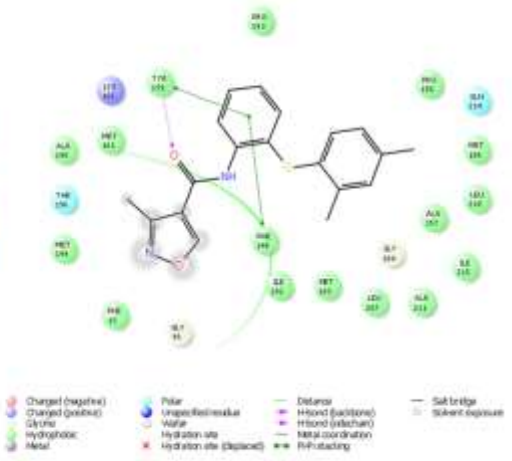

2D view of binding of compound **6n**

In silico absorption, distribution, metabolism, and excretion (ADME) properties of the newly synthesized bicyclic [2-(2,4-dimethylphenylthio)phenyl] aniline analogues were calculated using a QikProp[19] embedded within the Maestro. Further, among the forty-four pharmaceutically relevant descriptors available in QikProp the descriptors like QPlogPo/w, QPlogS, QPPCaco, QPlogBB, QPlogKhsa and % human oral absorption were calculated and presented in **Table S6**. For all these derivatives, the partition coefficient (QPlogPo/w) and water solubility (QPlogS) critical for estimating the absorption and distribution of drugs within the body ranged between 6.782 to 4.183 and -4.557 to -5.404 respectively. The blood-brain barrier partition coefficient (QPlogBB) ranged from 0.406 to -0.595. QPPCaco and QPlogKhsa varied from 6119.414 to 422.22 and 1.450 to 0.362 respectively. Further, the percentage human oral absorption was found to be 100% for all the compounds. Also, follow both the Lipinski's rule of five and Jorgensen's rule of three. Hence, from the pharmacokinetic parameters it was observed that all the properties were within the acceptable range which is defined for human use which revealed their potential of having possible drug-like properties.

The docking study further proposed bicyclic [2-(2, 4-dimethylphenylthio) phenyl] aniline analogues have significant active binding site of InhA. Thus for Docking score of most active compounds **6j** and **6n** was found to be -9.964, and -10.027.It suggests that mechanism of action for the antitubercular activity of these compounds might be through inhibition of mycobacterial enzyme InhA. Further, in silico ADME properties were predicted which suggested that all the active compounds was suitable for human use through oral absorption and possessing drug like properties. All these study make these compounds valid lead for further optimization as potential antituberculosis agents.

Glidewas used for docking studies to examine the binding mode of bicyclic [2-(2,4-dimethylphenylthio)phenyl] aniline and its derivatives with the crystal structure of

Mycobacterium tuberculosis enoyl-acyl carrier protein reductase (InhA) (PDB ID: 4TZK). The ligands were prepared using LigPrep. The protein was refined using the protein preparation wizard present in Maestro. All the water molecules were deleted. H-atoms were added to the protein, including the protons necessary to define the correct ionization and tautomeric states of the amino acid residues. Prime interface module incorporated in Maestro was used to add the missing residues of the side chain. Each structure minimization was carried out with the impact refinement module, using the OPLS-2005 force field to alleviate steric clashes potentially existing in the structures. Minimization was terminated when the energy converged, or the root mean square deviation reached a maximum cut-off of 0.30 Å.The grid was prepared using grid generation panel of glide with the default settings to find out an active site.The gridwas prepared for defining the binding site of the native ligand on the receptor. The ligand was selected to define the position and size of the active site. The results of docking studies were analyzed using Site Map.

1.7 ADME study

In silico absorption, distribution, metabolism, excretion (ADME) and drug likeness analysis

Table S7. ADME properties of the synthesized bicyclic [2-(2, 4-dimethylphenylthio) phenyl] aniline derivatives.

Entry	**QPlogPo/w**	**QPlogS**	**QPPCaco**	**QPlogBB**	**QPlogKhsa**	**Percent Human Oral Absorption**	**Rule Of Five**	**Rule Of Three**
6a	4.542	-4.447	4520.938	0.13	0.517	100	0	0
6b	4.828	-5.328	4546.243	0.406	0.623	100	0	0
6c	4.958	-5.003	5385.353	0.156	0.739	100	0	0

6d	4.428	-5.021	4629.268	0.063	0.6	100	0	0
6e	5.016	-4.936	5299.932	0.027	0.771	100	1	0
6f	4.451	-5.43	1754.701	-0.445	0.655	100	0	0
6g	5.443	-5.792	6119.414	0.18	0.999	100	1	1
6h	6.782	-6.928	3666.871	-0.121	1.45	100	1	1
6i	5.145	-4.575	4455.957	0.018	0.858	100	1	0
6j	5.684	-6.669	1524.322	-0.595	1.127	100	1	1
6k	4.183	-4.53	2782.727	-0.102	0.52	100	0	0
6l	4.733	-4.93	4192.14	0.037	0.638	100	0	0
6m	4.698	-4.557	422.2	-0.362	0.362	100	0	0
6n	4.24	-5.708	1252.732	-0.586	0.666	100	0	1
6o	5.416	-5.404	4767.221	0.344	0.85	100	1	0

QPlogPo/w: Predicted octanol/water partition coefficient (-2.0 to 6.5)

QPlogS: Predicted aqueous solubility in mol dm-3 (-6.5 to 0.5)

QPPCaco: Predicted apparent Caco-2 cell (gut-blood barrier model) permeability in nm/sec (< 25 poor; > 500 excellent)

QPlogBB: Predicted brain/blood partition coefficient (-3 to 1.2)

QPlogKhsa: Prediction of binding to human serum albumin (-1.5 to 0.5)

% Human oral absorption: Predicted human oral absorption (< 25 poor; > 80 high)

Rule Of Five: Number of violations of Lipinski's rule of five. (Maximum is 4)

Rule Of Three: Number of violations of Jorgensen's rule of three. (Maximum is 3)

2. Spectral data

2.1 2, 4 Dimethyl Thiophenol (2):

^{1}H NMR of 2, 4 Dimethyl Thiophenol (2)

^{1}H NMR ($CDCl_3$): δ=2.27 (s, 3H), 2.30 (s, 3H), 3.20(s, SH), 6.88 (d, J= 8.0Hz, 1H), 6.99 (s, 1H) and 7.17 (d, J=8.0Hz, 1H) ppm.

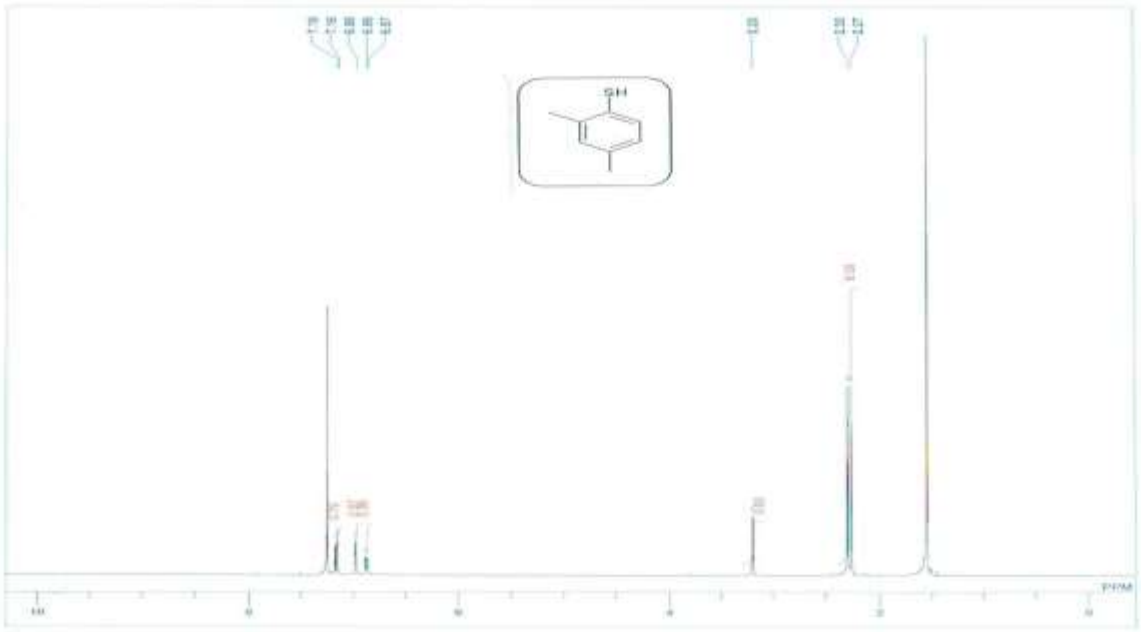

^{13}C NMR of 2, 4 Dimethyl Thiophenol (2)

^{13}C NMR ($CDCl_3$): δ= 20.79, 20.97, 126.86, 127.26, 130.27, 131.15, 135.77 and 136.22 ppm.

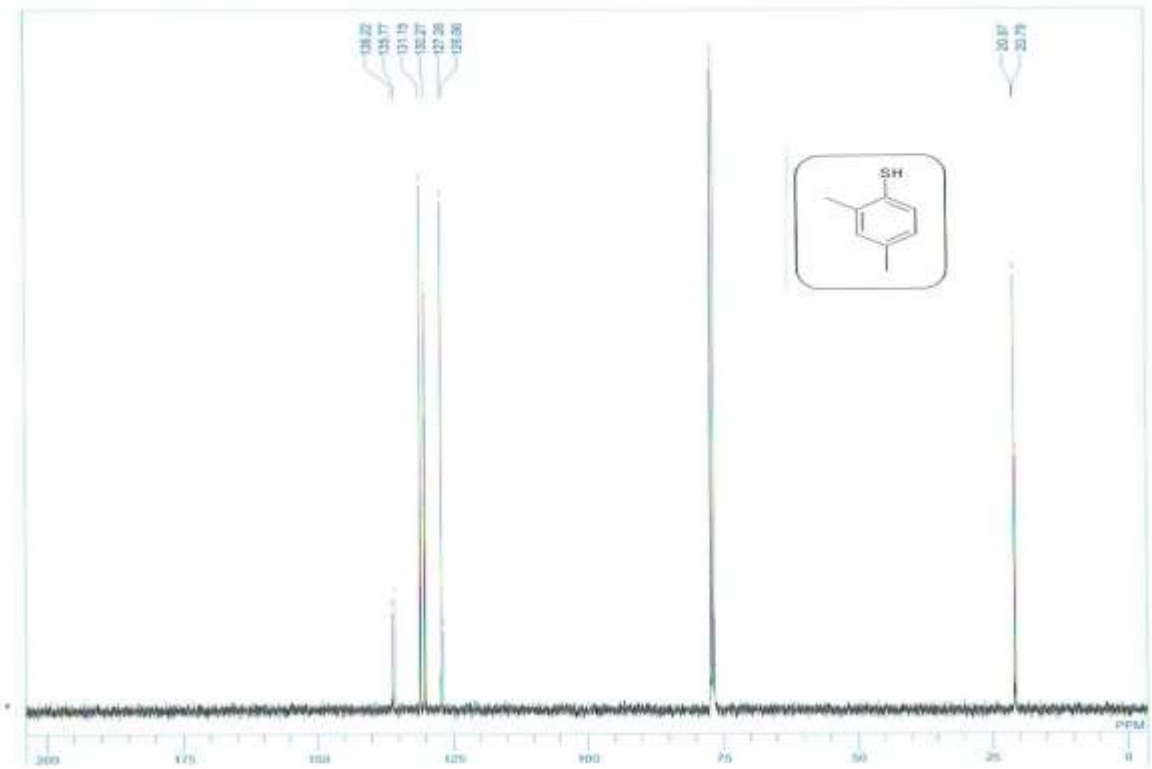

MS(EI) calculated for $C_8H_{10}S$ $[M-H]^+$: 137.1; found 137.2.

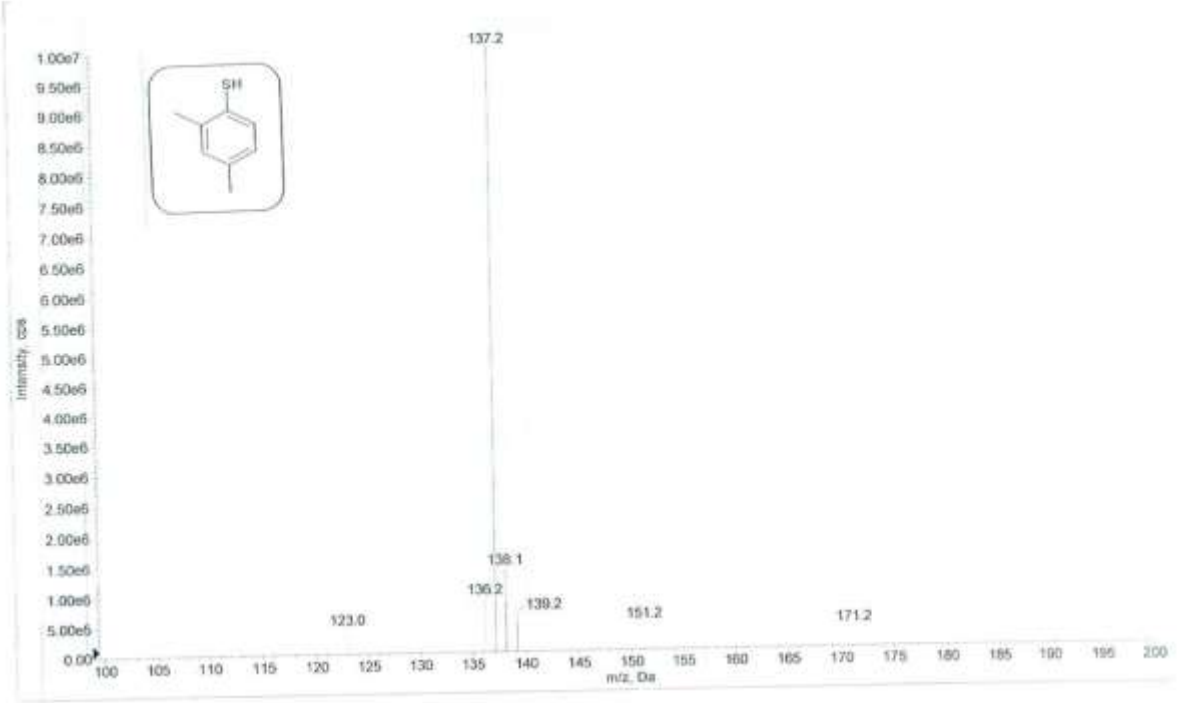

2.1 (2,4-dimethylphenyl)(2-nitrophenyl)sulfane(4):

^{1}H NMR of (2, 4-dimethylphenyl) (2-nitrophenyl) sulfane (4)

^{1}H NMR ($CDCl_3$): δ=2.36 (s, 3H), 2.45(s, 3H), 6.76(dd, J=8.0Hz, 1H), 7.17 (d, J= 7.0Hz, 1H), 7.26 (m, 2H), 7.36 (m, 1H), 7.52 (d, J=8.0Hz, 1H) and 8.31 (dd, J=8.0, 1H) ppm.

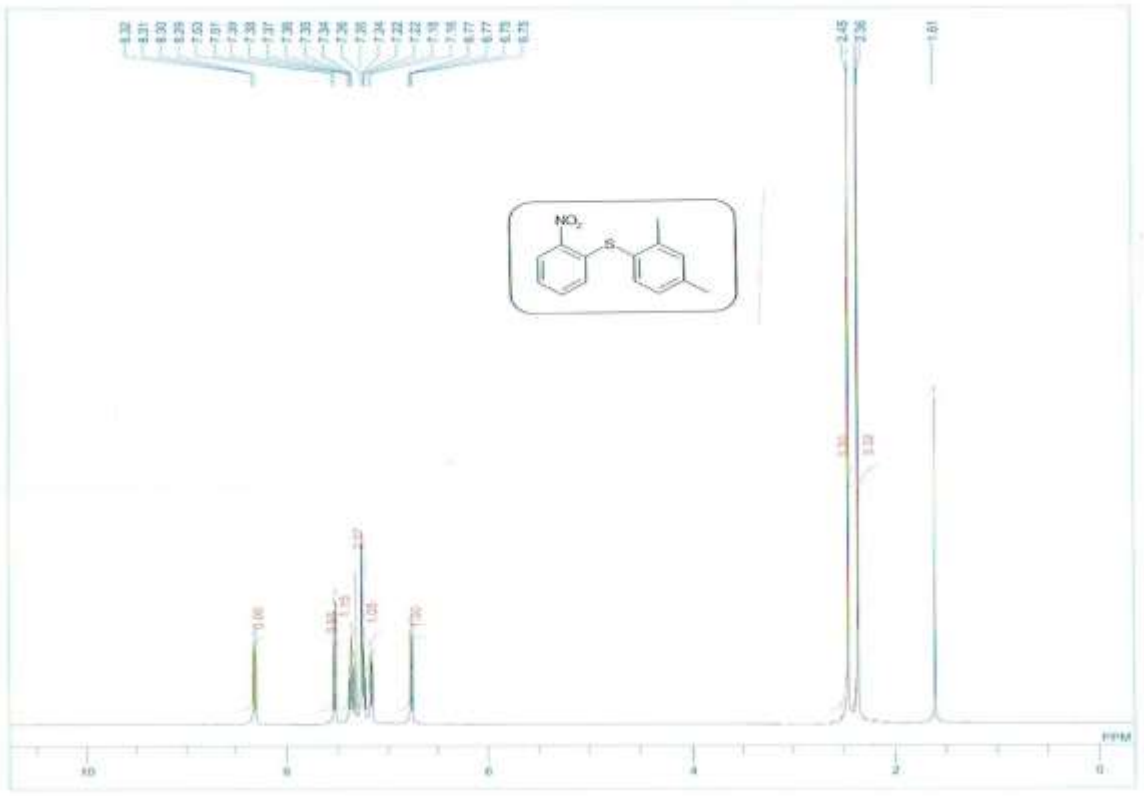

^{13}C NMR of (2, 4-dimethylphenyl) (2-nitrophenyl) sulfane (4)

^{13}C NMR ($CDCl_3$): δ= 19.98, 20.73, 115.01, 115.24, 118.78, 126.49, 127.26, 130.41, 131.13, 131.68, 135.28, 135.71, 136.55 and 148.13 ppm.

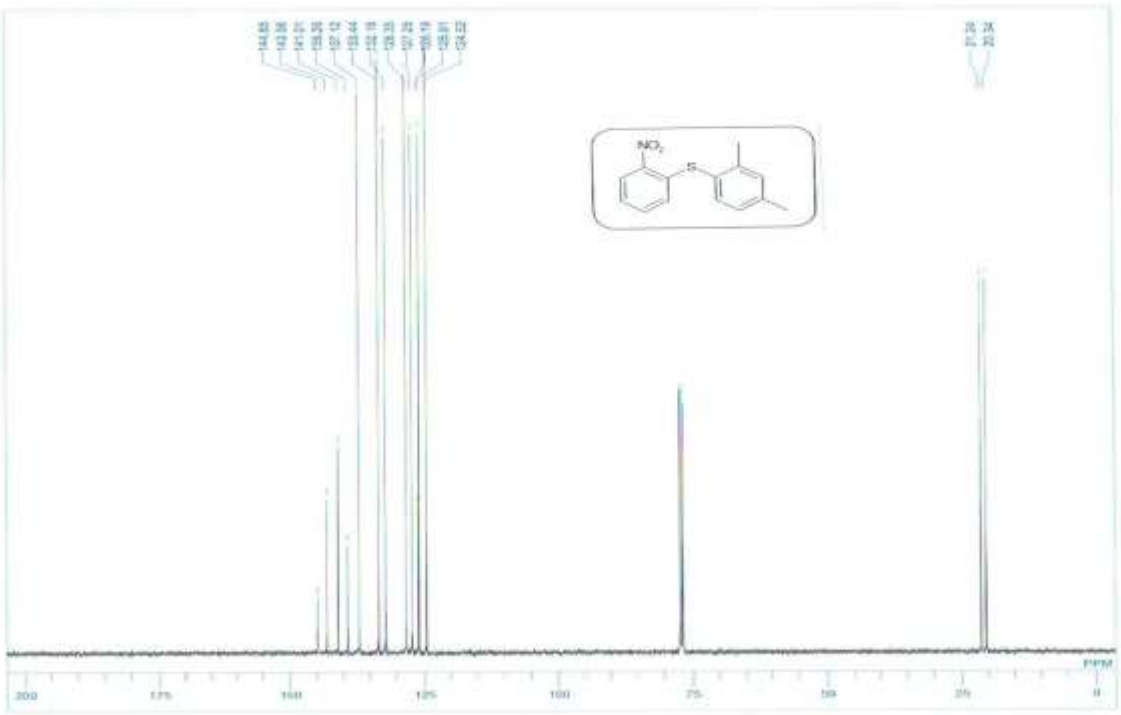

MS(EI) calculated for $C_{14}H_{13}NO_2S$ $[M+H]^+$: 260.1; found 260.0.

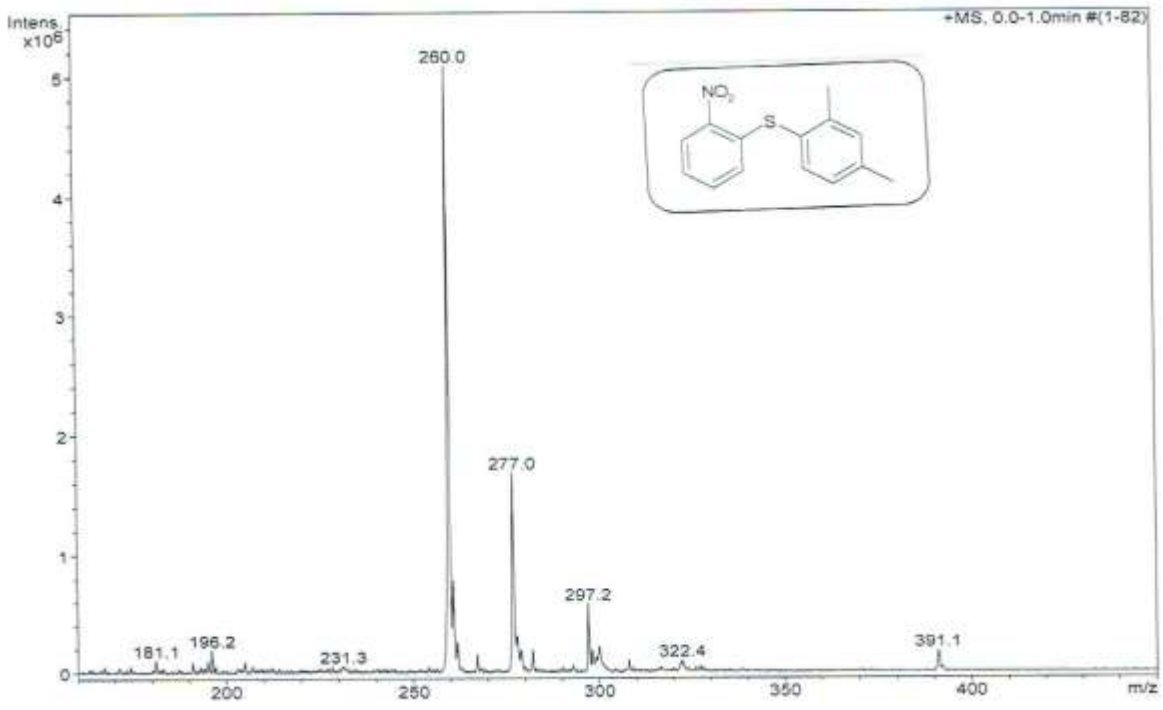

2.3 2-(2, 4-dimethylphenylthio) benzenamine (5):

^{1}H NMR of 2-(2, 4-dimethylphenylthio) benzenamine (5)

^{1}H NMR ($CDCl_3$): δ=2.26 (s, CH_3), 2.39(s, CH_3), 4.22 (s, NH_2), 6.69(d, J=8.0 Hz, Ar-H), 6.73-6.80 (m, Ar-2H), 6.85 (d, J=8.0 Hz, Ar-H), 7.00 (s, Ar-H), 7.19-7.23 (m, Ar-H) and 7.36 (dd, J=7.0 Hz, Ar-H) ppm

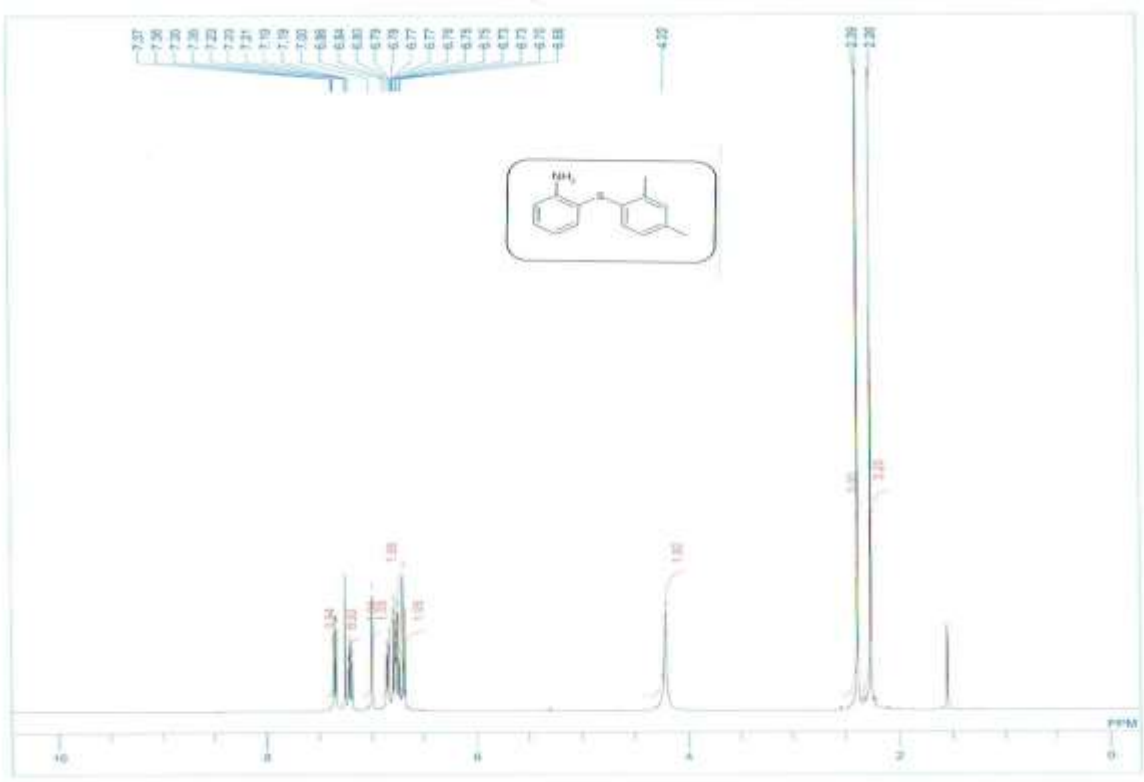

^{13}C NMR of2-(2, 4-dimethylphenylthio) benzenamine (5)

^{13}C NMR ($CDCl_3$): δ= 19.98, 20.73, 115.01, 115.24, 118.78, 126.49, 127.26, 130.41, 131.13, 131.68, 135.28, 135.71, 136.55 and 148.13 ppm.

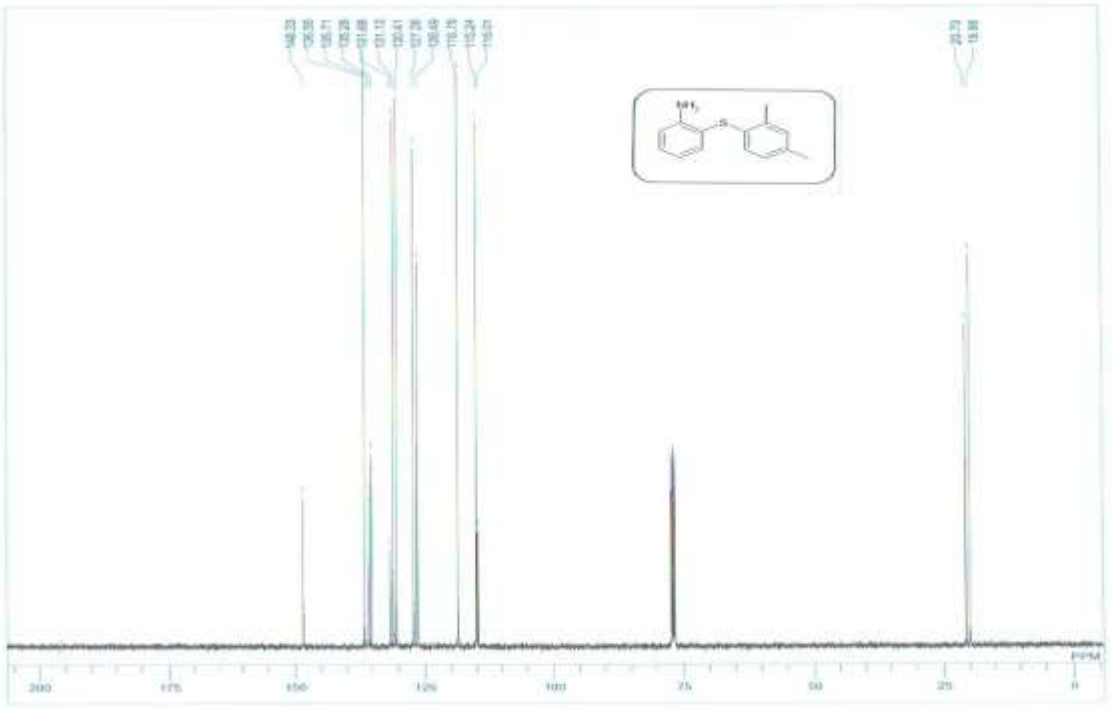

MS(EI) calculated for $C_{14}H_{15}NS$ $[M+H]^+$: 230.1; found 230.0.

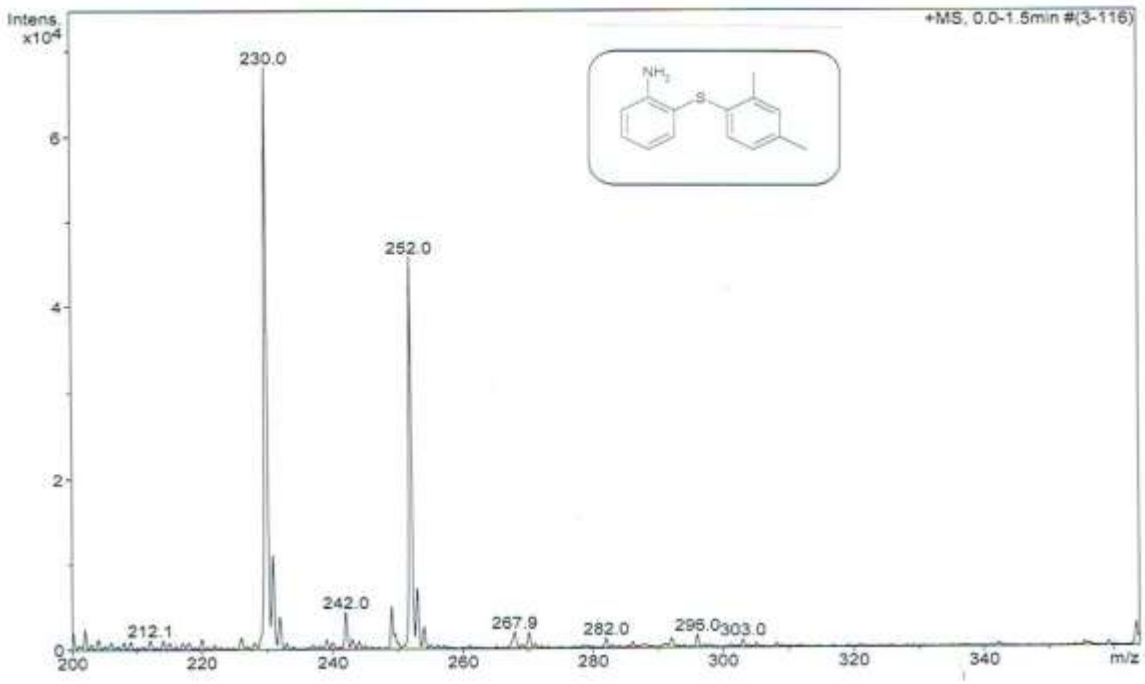

2.4 N-(2-(2, 4-dimethylphenylthio) phenyl) acetamide (6a):

^{1}H NMR of N-(2-(2, 4-dimethylphenylthio) phenyl) acetamide (6a)

^{1}H NMR (DMSO-d_6): δ=2.08 (s, CH_3), 2.28(s, CH_3), 2.39 (s, CH_3), 6.72 (d, J=7.0 Hz, Ar-H), 6.87 (d, J=7.0 Hz, Ar-H), 7.06 (m, Ar-2H), 7.39 (q, J=8.0 Hz, Ar-2H), 8.06 (s, NH) and 8.39(d, J=8.0 Hz, Ar-H) ppm.

^{13}C NMR of N-(2-(2, 4-dimethylphenylthio) phenyl) acetamide (6a)

^{13}C NMR (DMSO-d_6): δ= 20.16, 20.78, 27.70, 120.93, 121.21, 124.44, 127.66, 128.31, 129.93, 130.51, 131.41, 135.03, 136.66, 139.19and 168.24 ppm.

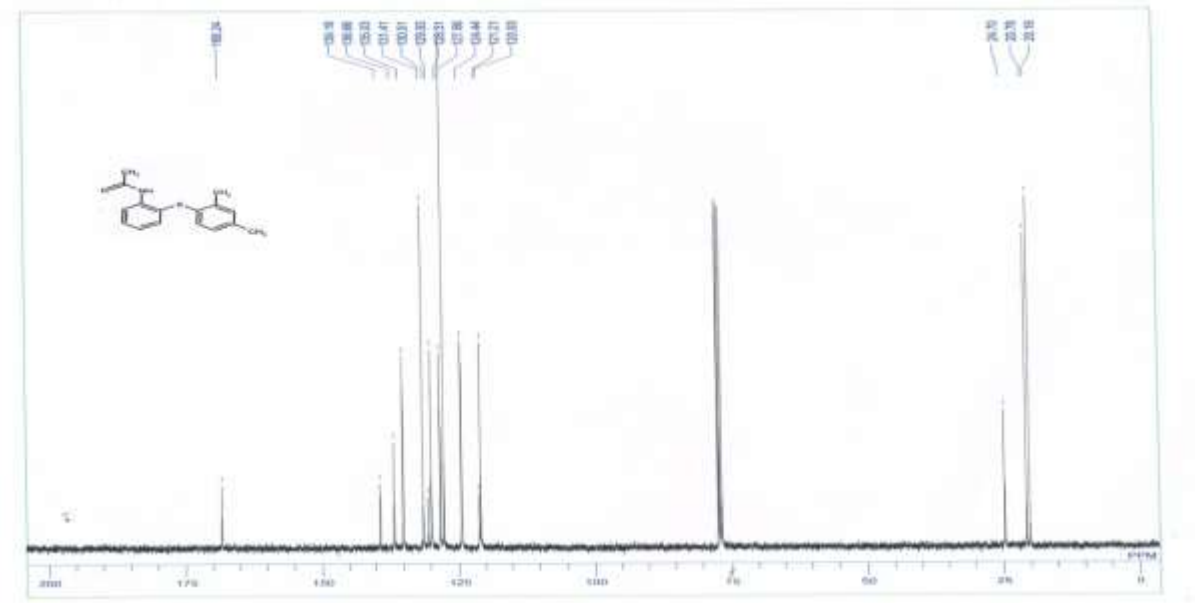

MS(EI) calculated for $C_{16}H_{17}NOS$ $[M+H]^+$: 272.1; found 272.1.

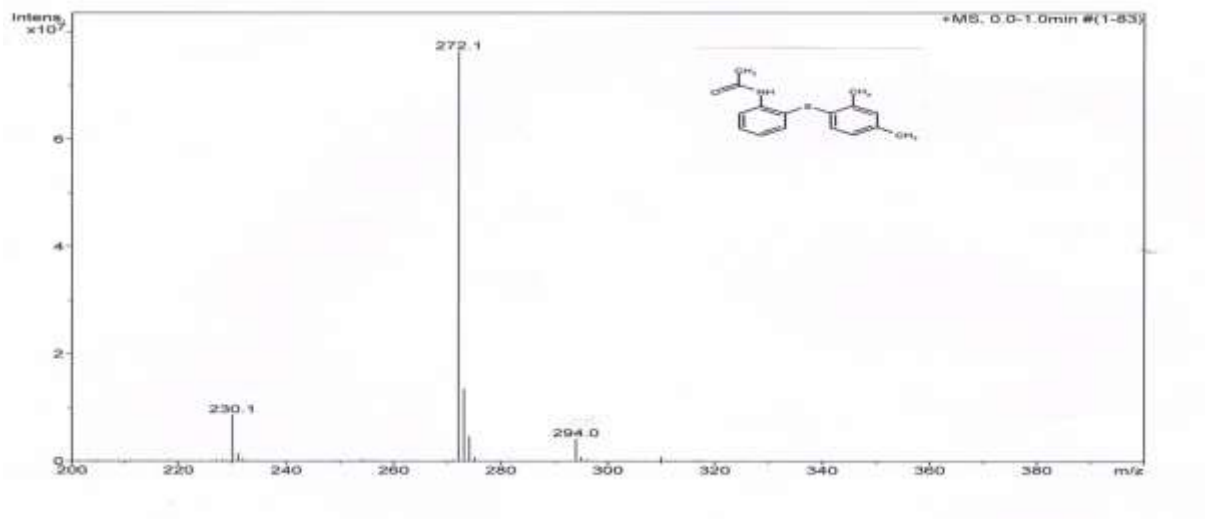

2.5 N-(2-(2, 4-dimethylphenylthio) phenyl)-2, 2, 2-trifluoroacetamide (6b)

*1*H NMR of N-(2-(2,4-dimethylphenylthio)phenyl)-2,2,2-trifluoroacetamide (6b**)**

^{1}H NMR (DMSO-d_6): δ=2.28(s, CH_3), 2.38 (s, CH_3), 6.75 (d, J=7.0 Hz, Ar-H), 6.88 (d, J=7.0 Hz, Ar-H), 7.04 (s, Ar-H), 7.22 (t, J=7.0 Hz, Ar-H), 7.45 (t, J=7.0 Hz, Ar-H), 7.51 (m, Ar-H), 8.35 (d, J=8.0 Hz, Ar-H) and 8.95(s, NH) ppm.

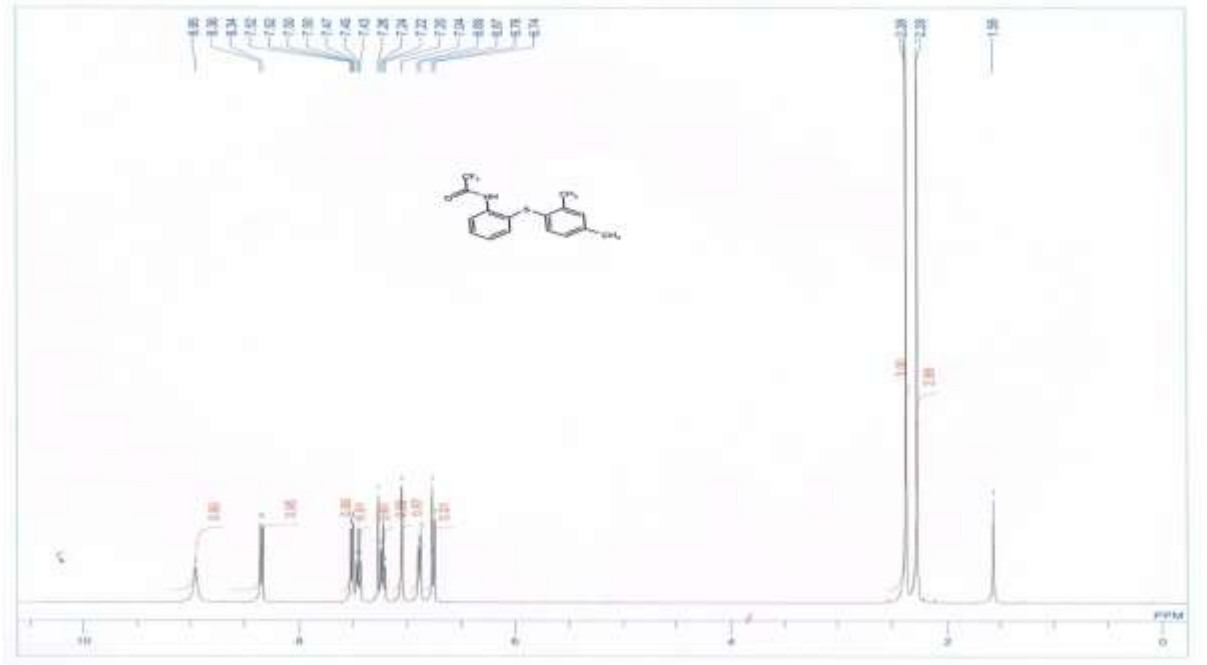

^{13}C NMR of N-(2-(2, 4-dimethylphenylthio) phenyl)-2, 2, 2-trifluoroacetamide (6b**)**

^{13}C NMR (DMSO-d_6): δ= 20.16, 20.82, 70.51, 114.12, 116.99, 121.16, 123.5, 126.44, 127.82, 128.94, 129.45, 130.09, 131.64, 135.38, 135.38, 136.27 and 137.31 ppm.

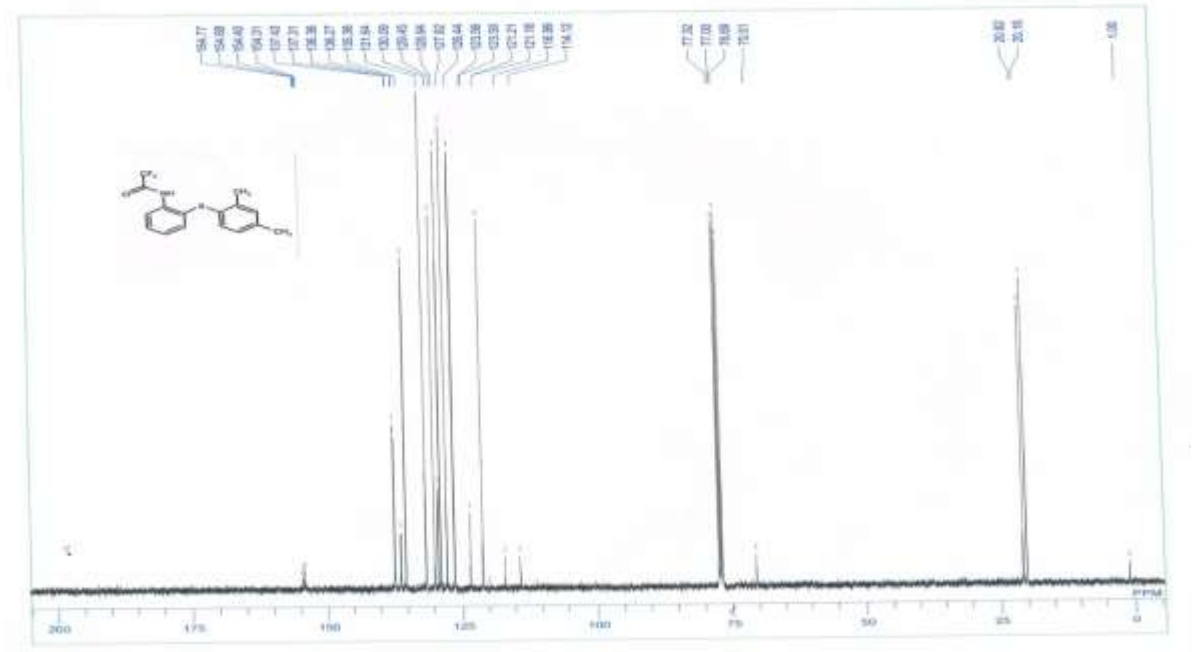

MS(EI) calculated for $C_{16}H_{14}F_3NOS$ $[M+H]^+$: 226.1; found 326.0.

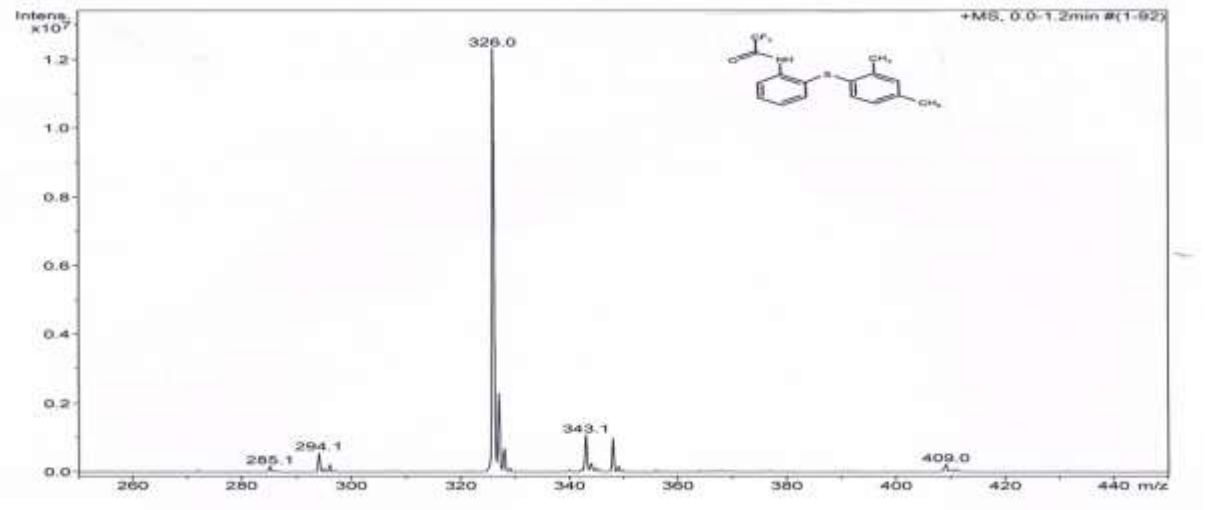

2.6 N-(2-(2, 4-dimethylphenylthio) phenyl) isobutyramide(6c)

^{1}H NMR of N-(2-(2, 4-dimethylphenylthio) phenyl) isobutyramide(6c)

^{1}H NMR (DMSO-d_6): δ=1.08 (s, CH_3), 1.10(s, CH_3), 2.26 (s, CH_3), 2.36-2.46 (m, CH_3 and CH), 6.65 (d, J=8.0 Hz, Ar-H), 6.84 (d, J=8.0 Hz, Ar-H), 7.02 (s, Ar-H), 7.08 (m, Ar-H), 7.38-7.46 (m, Ar-2H), 8.16 (s, NH) and 8.45(d, J=8.0 Hz, Ar-H) ppm.

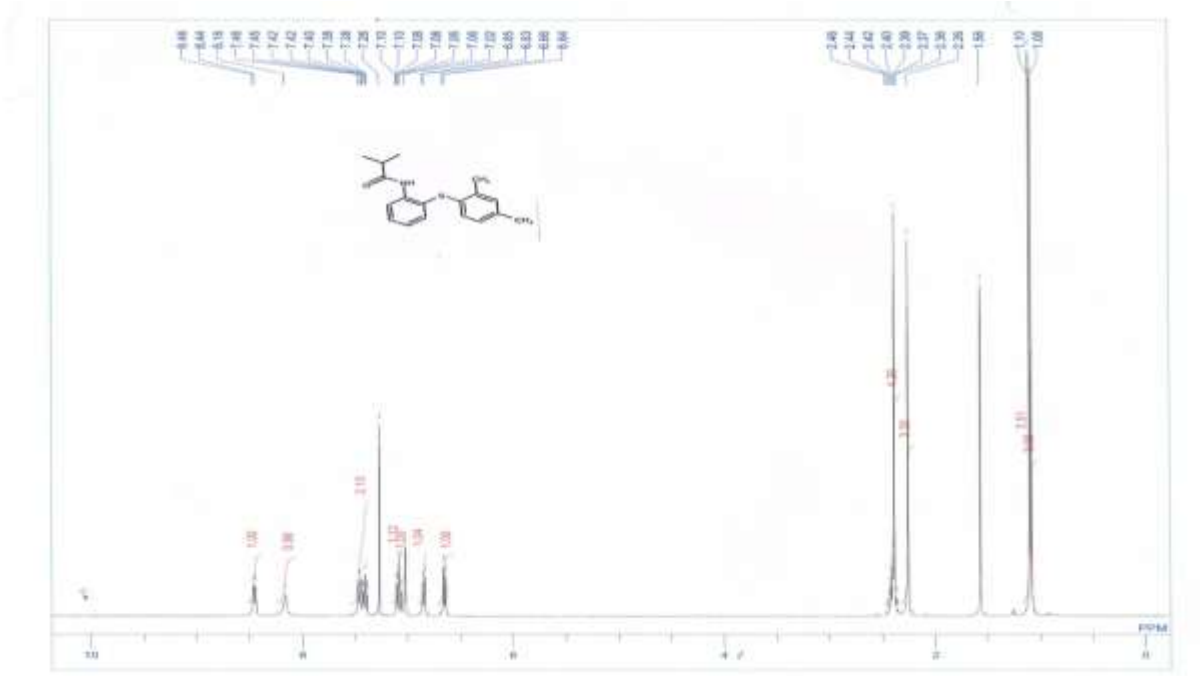

^{13}C NMR of N-(2-(2, 4-dimethylphenylthio) phenyl) isobutyramide(6c)

^{13}C NMR (DMSO-d_6): δ= 19.26, 20.10, 20.77, 36.92, 120.77, 124.26, 127.52, 127.69, 130.26, 130.59, 131.35, 135.48, 136.14, 136.37, 139.46 and 175.07 ppm.

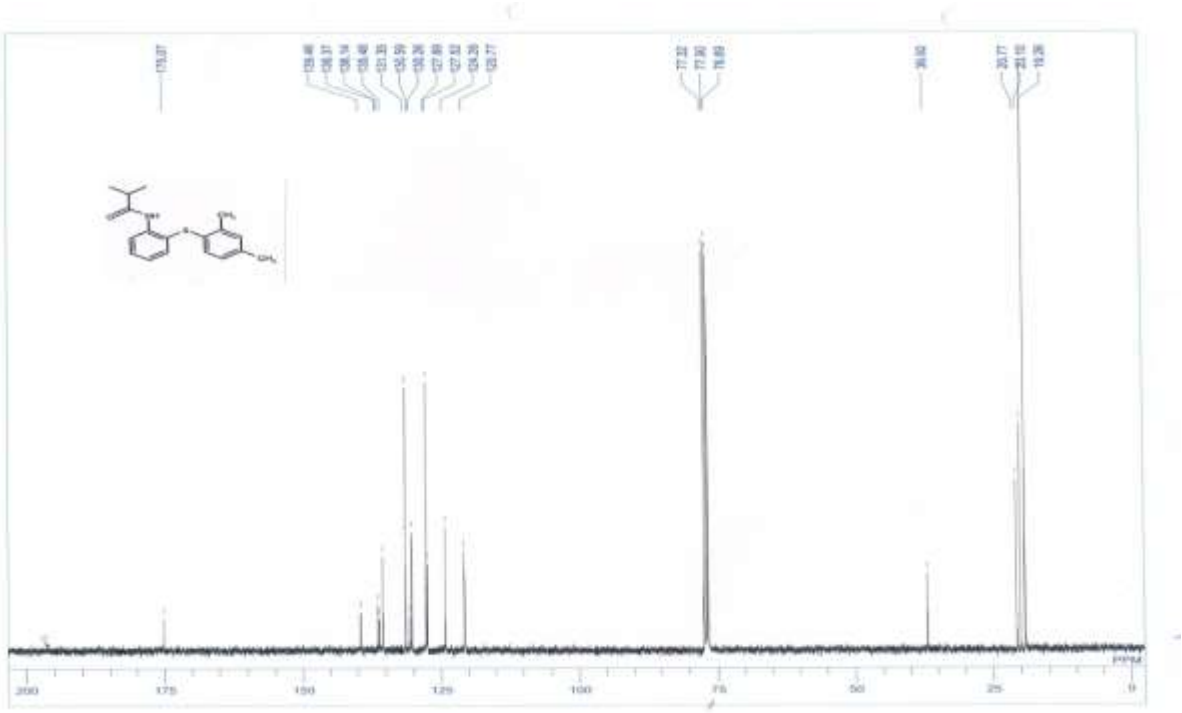

MS(EI) calculated for $C_{17}H_{19}NOS$ $[M+H]^+$: 300.1; found 300.2.

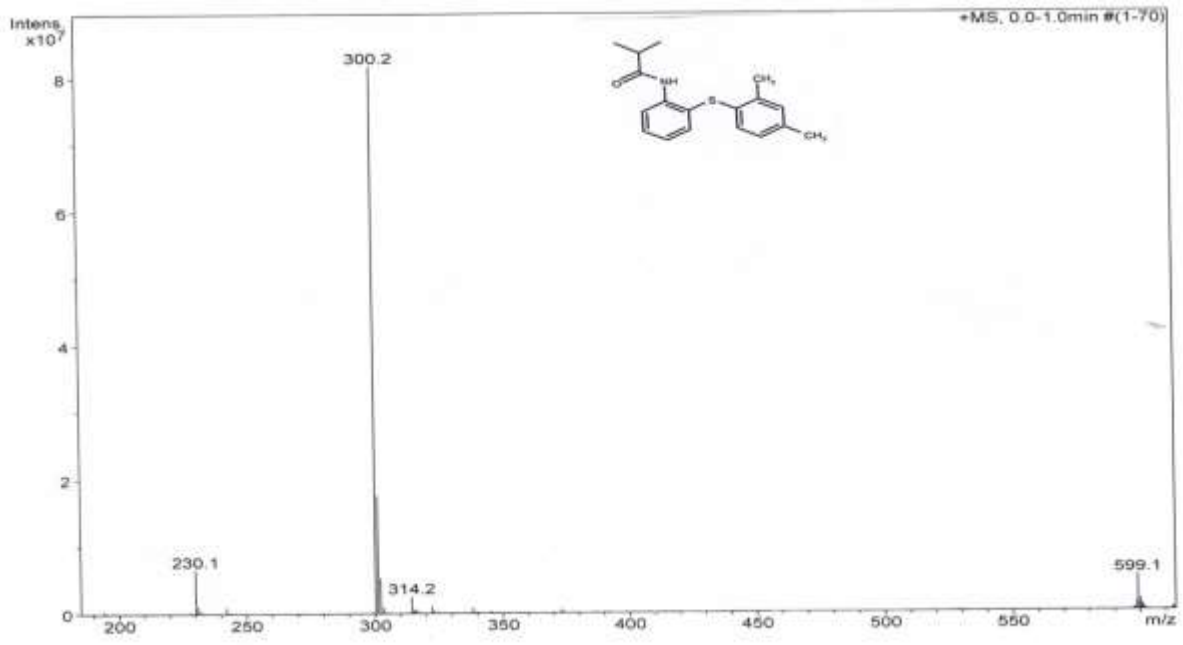

2.7 N-(2-(2, 4-dimethylphenylthio) phenyl) propionamide (6d)

^{1}H NMR of N-(2-(2, 4-dimethylphenylthio) phenyl) propionamide (6d)

^{1}H NMR (DMSO-d_6): δ=1.06 (t, CH_3), 2.20-2.31 (m, CH_3 and CH_2), 6.90 (d, J=7.0 Hz, Ar-H), 7.0 (d, J=7.0 Hz, Ar-H), 7.07-7.10 (m, Ar-2H), 7.15 (s, Ar-H), 7.30 (t, J=8.0 Hz, Ar-H),

7.37 (m, Ar-H), and 9.30(s, NH) ppm.

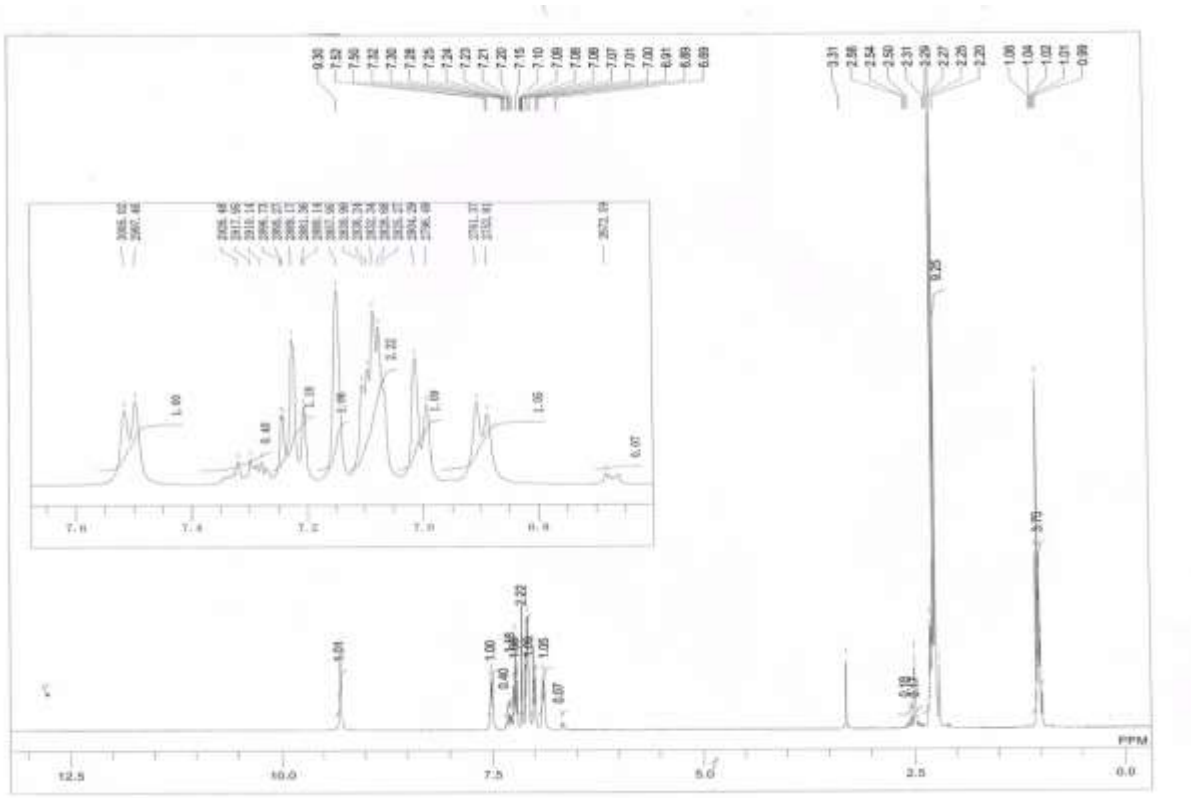

^{13}C NMR of N-(2-(2, 4-dimethylphenylthio) phenyl) propionamide (6d)

^{13}C NMR (DMSO-d_6): δ= 9.76, 20.05, 20.77, 126.03, 127.17, 127.82, 129.58, 130.23, 131.62, 132.83, 135.90, 136.63, 138.04, 139.55, 141.68 and 175.50 ppm.

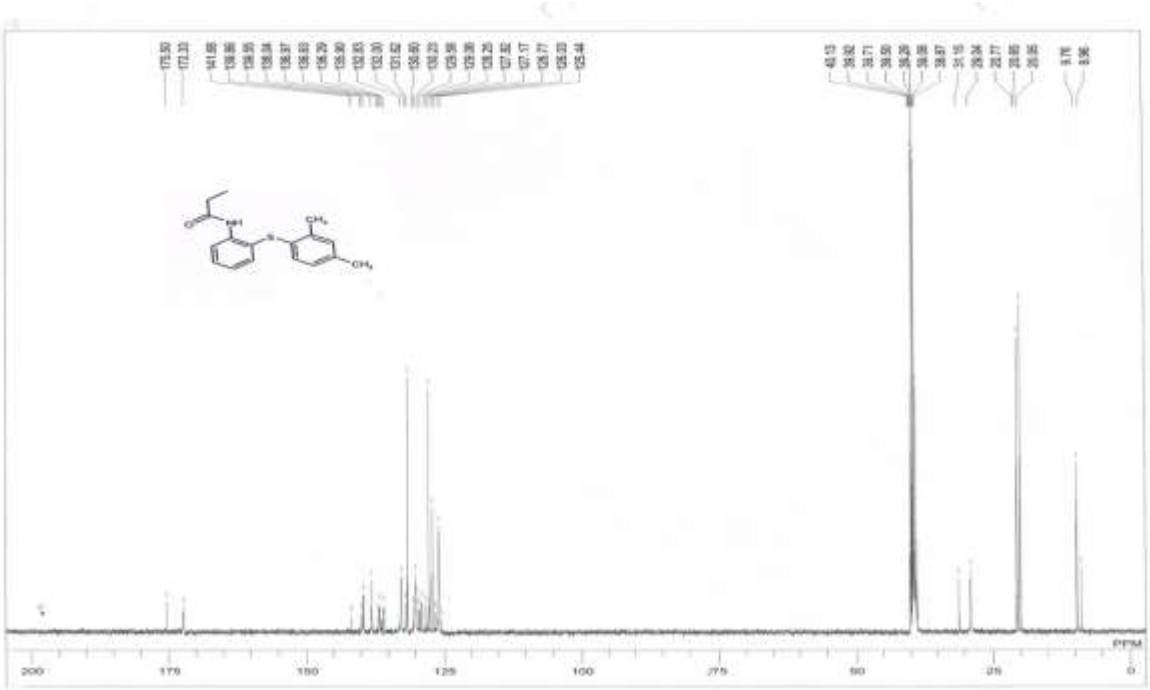

MS(EI) calculated for $C_{17}H_{19}NOS$ $[M+H]^+$: 286.1; found 286.2.

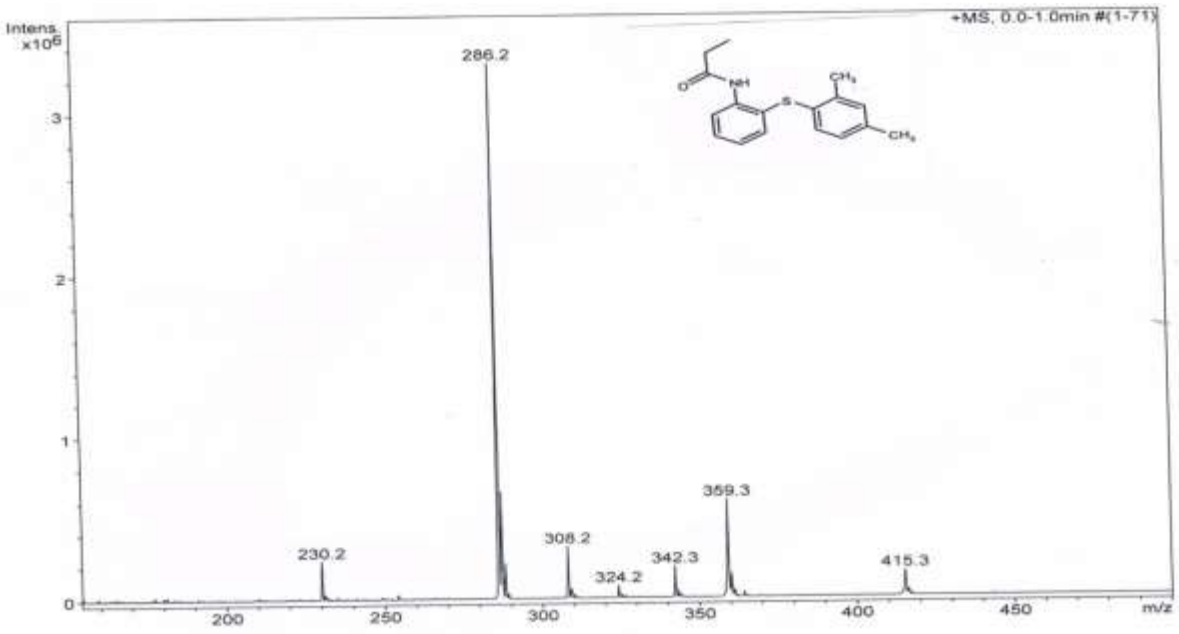

2.8 N-(2-(2, 4-dimethylphenylthio) phenyl) pentanamide (6e)

^{1}H NMR of N-(2-(2, 4-dimethylphenylthio) phenyl) pentanamide (6e)

^{1}H NMR (DMSO-d_6): δ=0.85 (t, J=7.0 Hz, CH_3), 1.27(m, J=7.0 Hz, CH_2), 1.52 (m, CH_2), 2.24 (t, CH_2), 2.26 (s, CH_3), 2.39 (s, CH_3), 6.67 (d, J=8.0 Hz, Ar-H), 6.85 (d, J=8.0 Hz, Ar-H), 7.02 (s, Ar-H), 7.08 (m, J=8.0 Hz, Ar-H), 7.38-7.45 (m, Ar-2H), 8.08 (s, NH) and 8.43(d, J=8.0 Hz, Ar-H) ppm.

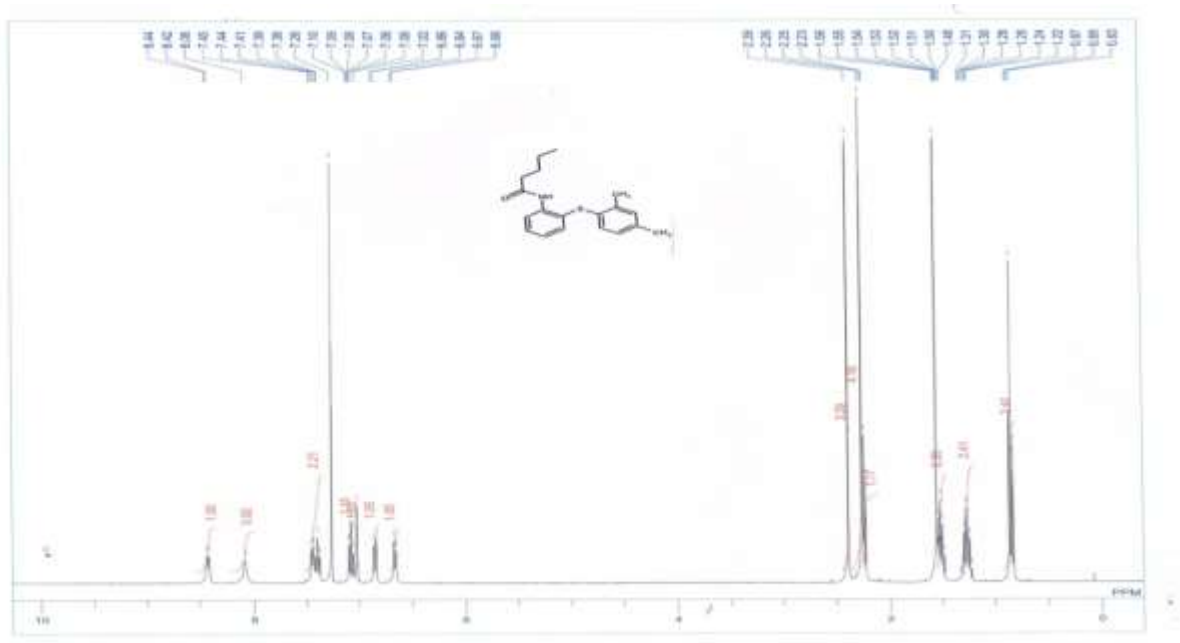

^{13}C NMR of N-(2-(2, 4-dimethylphenylthio) phenyl) pentanamide (6e)

^{13}C NMR (DMSO-d_6): δ= 13.69, 20.14, 20.78, 22.20, 27.49, 37.80, 120.84, 124.31, 127.71, 127.78, 130.18, 130.64, 131.39, 135.39, 136.32, 136.46, 139.39 and 171.38 ppm.

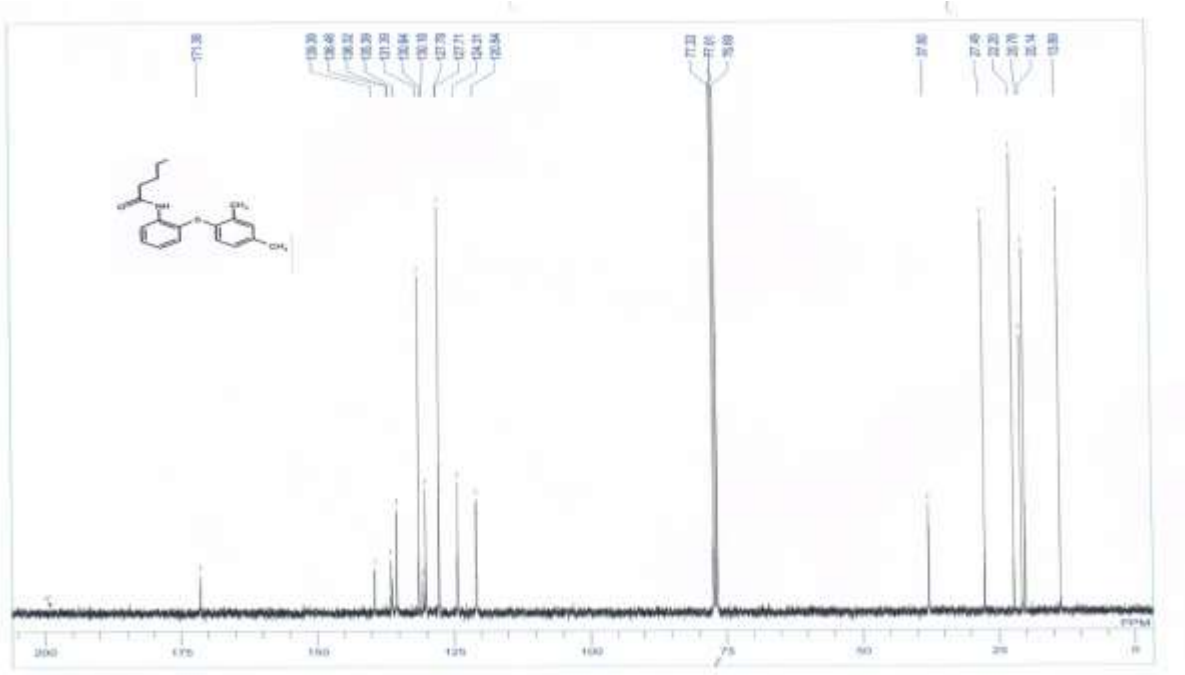

MS(EI) calculated for $C_{19}H_{23}NOS$ $[M+H]^+$: 314.2; found 314.3.

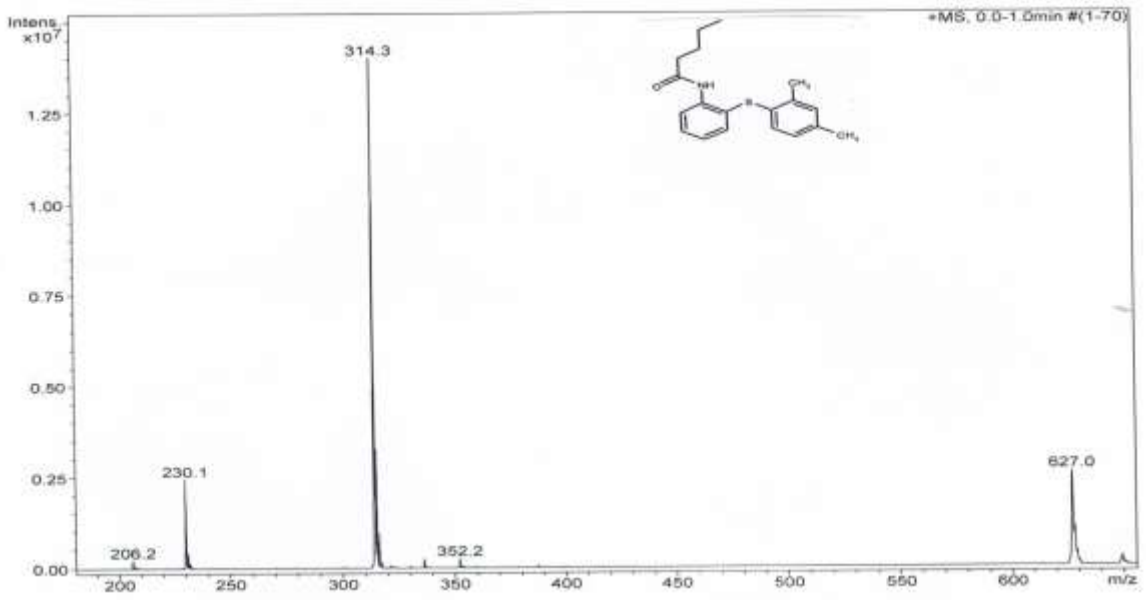

2.9 ethyl (2-(2, 4-dimethylphenylthio) phenylcarbamoyl) formate (6f)

^{1}H NMR of ethyl (2-(2, 4-dimethylphenylthio) phenylcarbamoyl) formate (6f)

^{1}H NMR (DMSO-d_6): δ=1.29 (t, J=7.0 Hz, CH_3), 2.25 (s, CH_3), 2.28(s, CH_3), 4.29(q, J=7.0 Hz, CH_2), 6.99 (m, Ar-2H), 7.14 (d, J=6.0 Hz, Ar-2H), 7.21 (t, J=8.0 Hz, Ar-H), 7.37 (t, J=6.0 Hz, Ar-H), 7.78 (d, J=8.0 Hz, Ar-H) and 10.26(s, NH) ppm.

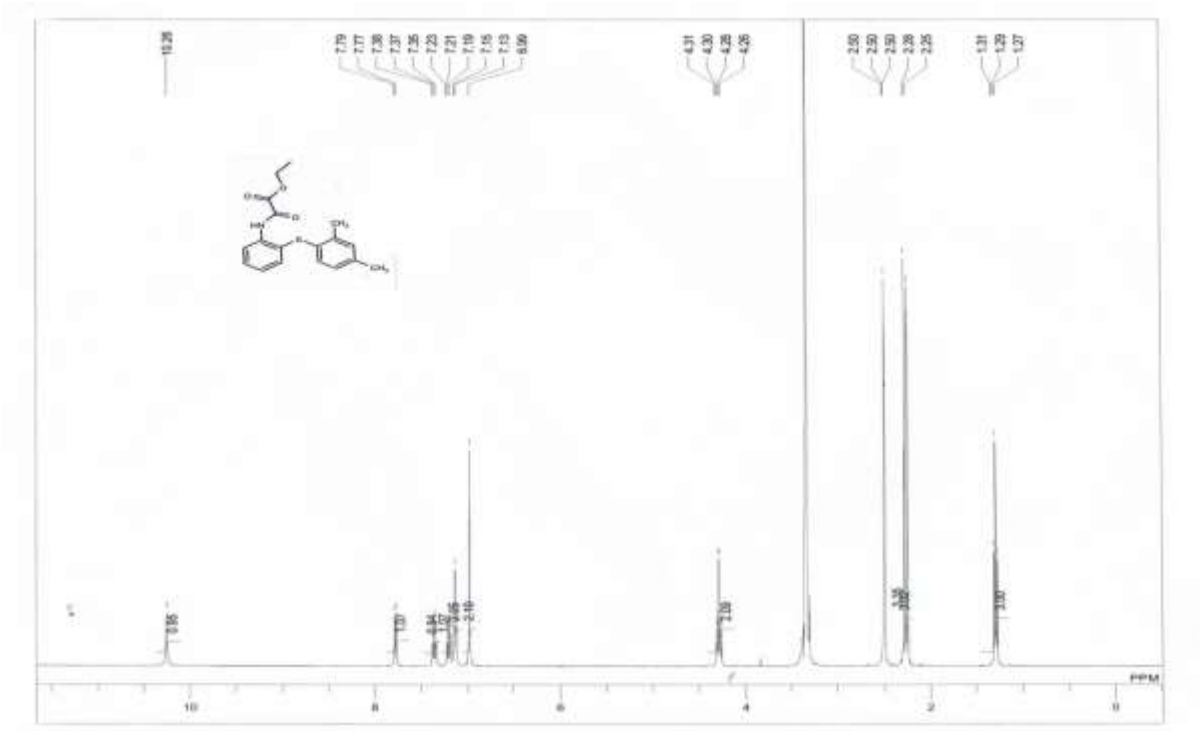

^{13}C NMR of ethyl (2-(2, 4-dimethylphenylthio) phenylcarbamoyl) formate (6f)

^{13}C NMR (DMSO-d_6): δ= 13.76, 19.92, 20.49, 62.69, 123.69, 126.75, 127.77, 128.22, 128.37, 129.02, 131.52, 132.12, 135.81, 137.65, 138.66, 154.96 and 160.17 ppm.

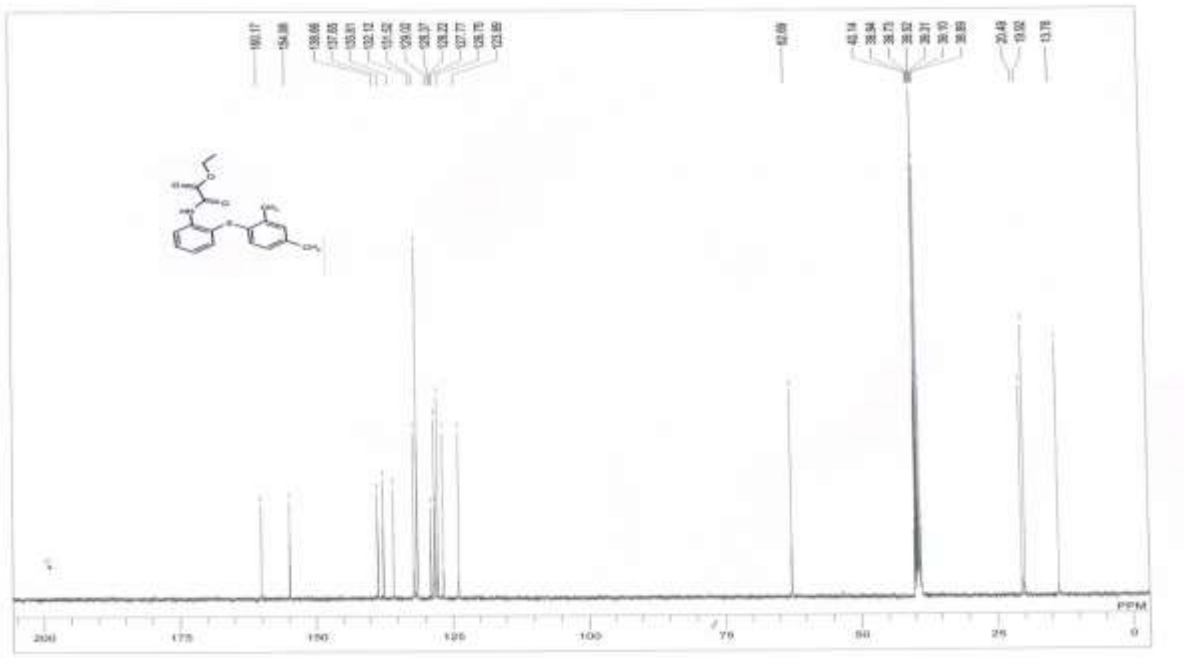

MS(EI) calculated for $C_{18}H_{19}NO_3S$ $[M+H]^+$: 330.1; found 330.1.

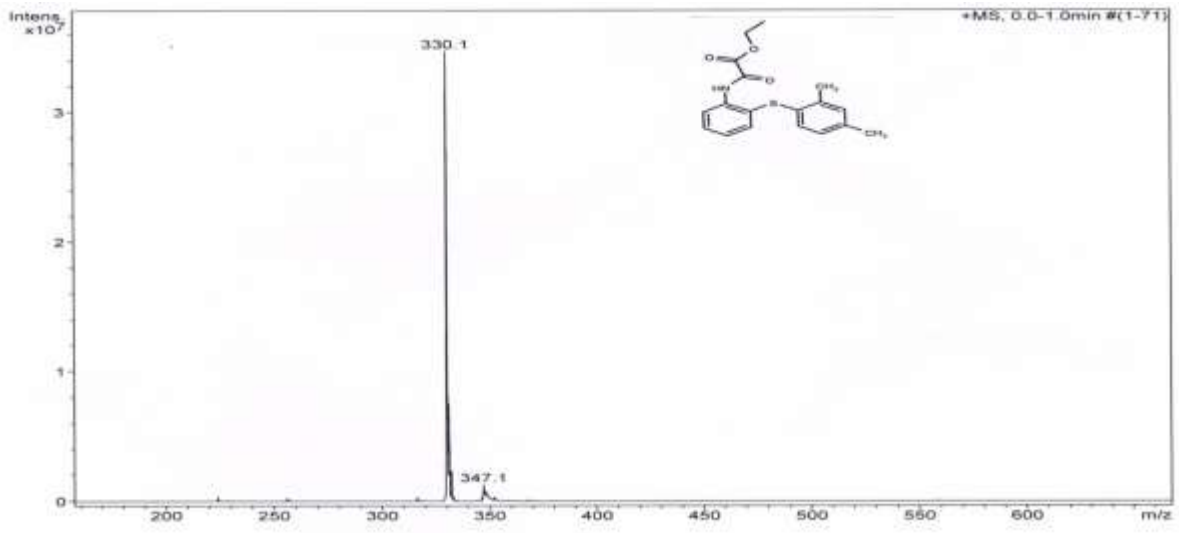

2.10 N-(2-(2, 4-dimethylphenylthio) phenyl) pivalamide (6g)

^{1}H NMR of N-(2-(2, 4-dimethylphenylthio) phenyl) pivalamide (6g)

^{1}H NMR (DMSO-d_6): δ=1.11 (s, 3CH_3), 2.25 (s, CH_3), 2.39 (s, CH_3), 6.56 (d, J=8.0 Hz, Ar-H), 6.82 (d, J=8.0 Hz, Ar-H), 7.01 (s, Ar-H), 7.09 (m, J=7.0 Hz & 1.5Hz, Ar-H), 7.40-7.44 (m, Ar-H), 7.48 (m, J=7.0Hz & 1.5Hz, Ar-H) and 8.44-8.49 (m, Ar-2H) ppm.

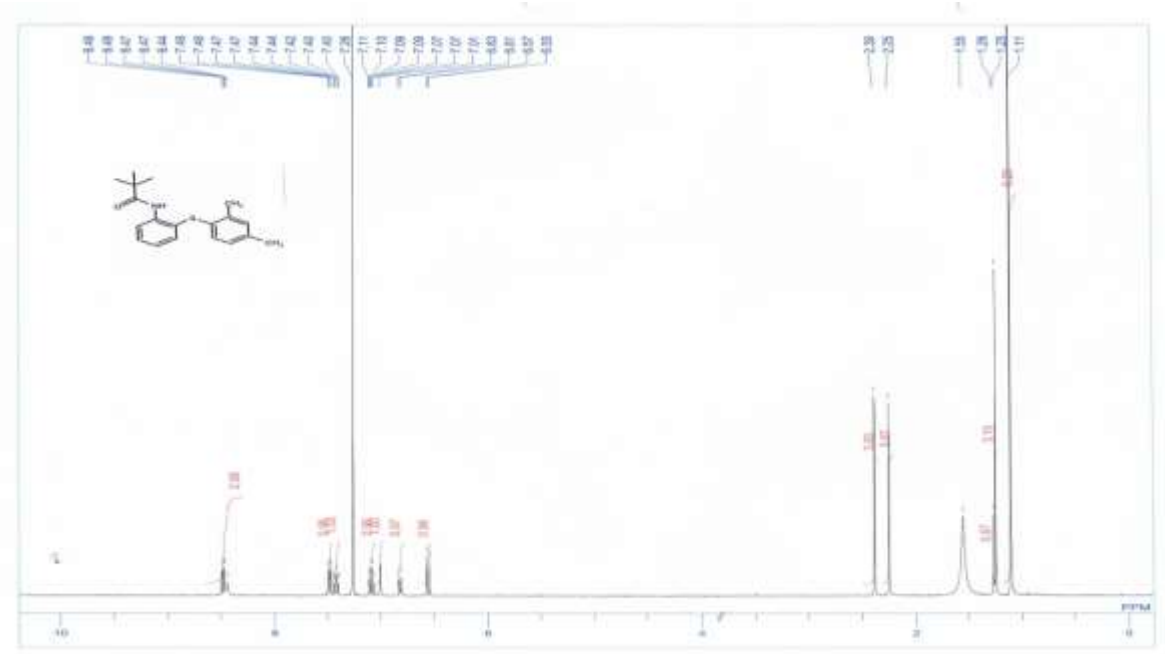

^{13}C NMR of N-(2-(2, 4-dimethylphenylthio) phenyl) pivalamide (6g)

^{13}C NMR (DMSO-d_6): δ= 19.96, 20.72, 27.20, 39.97, 120.39, 120.62, 124.18, 126.60, 127.66, 130.45, 130.57, 131.27, 135.54, 135.75, 136.04, 139.64 and 176.64 ppm.

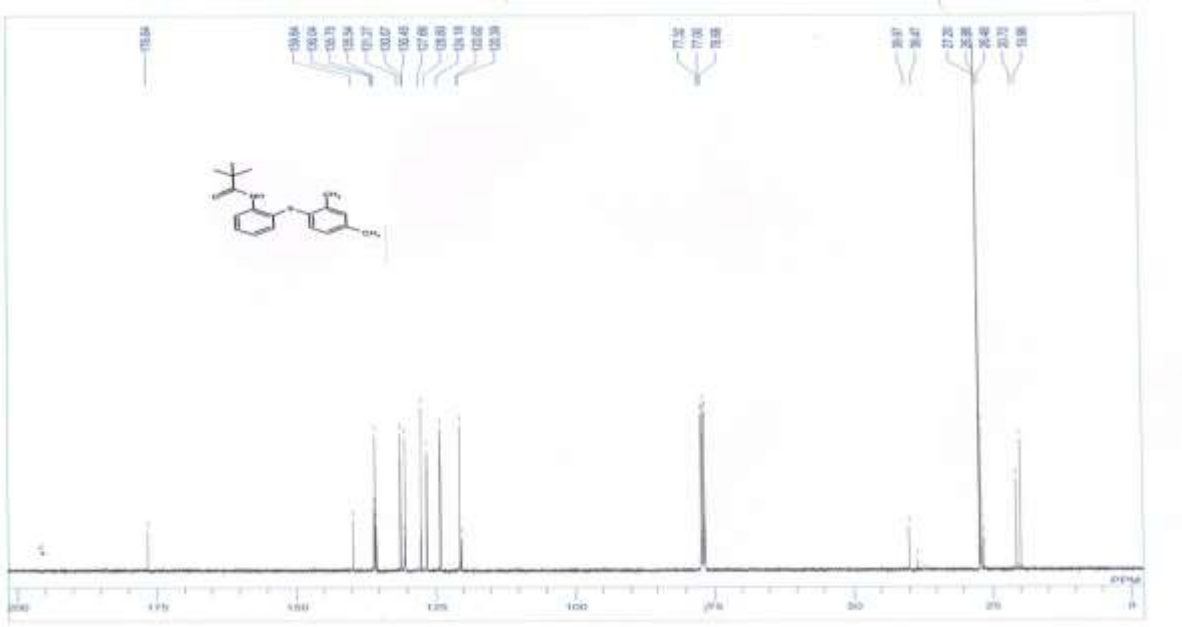

MS(EI) calculated for $C_{19}H_{23}NOS$ $[M+H]^+$: 314.4; found 314.3.

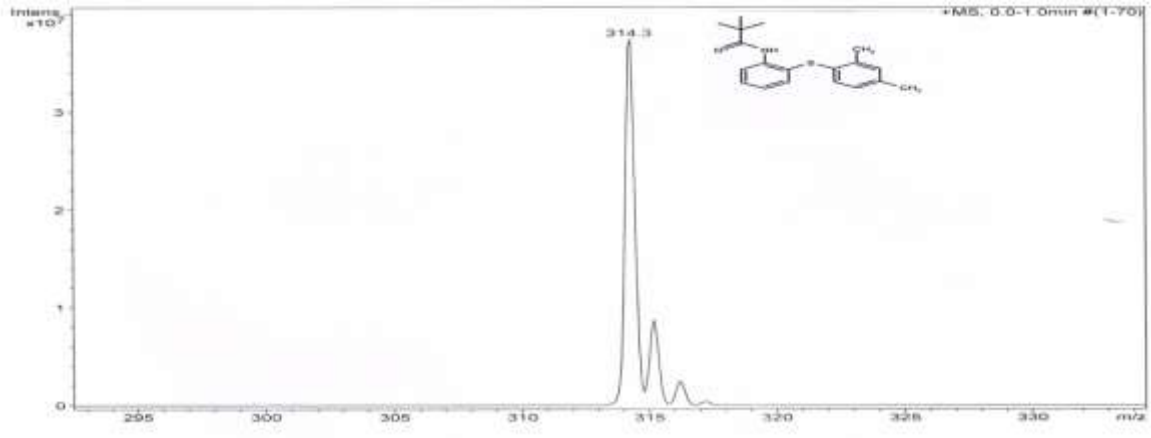

2.11 N-(2-(2, 4-dimethylphenylthio) phenyl) benzamide (6h)

^{1}H NMR of N-(2-(2, 4-dimethylphenylthio) phenyl) benzamide (6h)

^{1}H NMR (DMSO-d_6): δ=2.34 (s, 2CH_3), 6.71 (d, J=7.0 Hz, Ar-H), 7.03-7.09 (m, Ar-4H), 7.15 (s, Ar-H), 7.33-7.40 (m, Ar-5H), 7.44 (dd, J=7.0 Hz, Ar-2H) and 7.91 (m, Ar-4H) ppm.

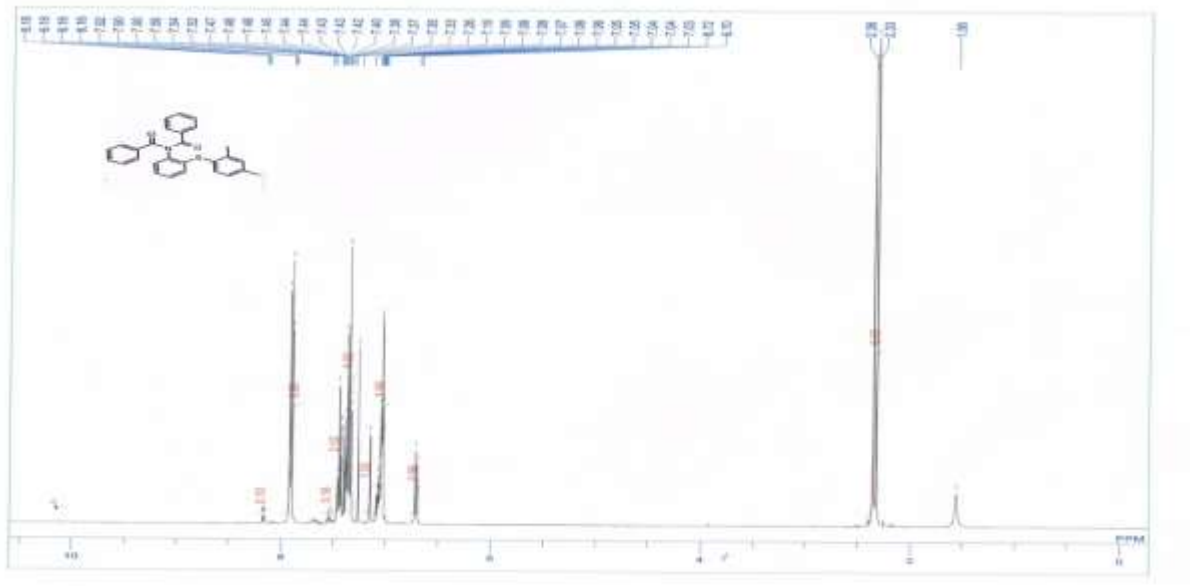

^{13}C NMR of N-(2-(2, 4-dimethylphenylthio) phenyl) benzamide (6h)

^{13}C NMR (DMSO-d_6): δ= 20.52, 21.10, 126.06, 126.30, 127.61, 127.89, 128.33, 128.73, 129.10, 129.73, 130.47, 131.85, 132.24, 134.83, 135.91, 136.76, 136.98, 139.69, and 142.07 ppm.

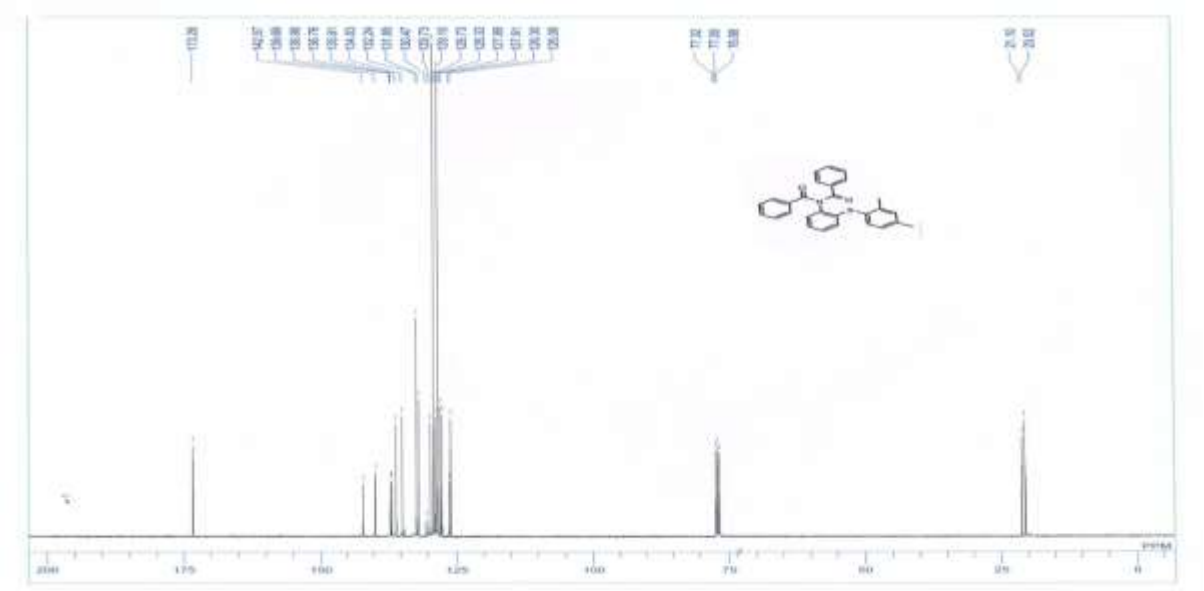

MS(EI) calculated for $C_{10}H_{17}N_3O_3$ $[M-H]^+$: 226.13; found 226.0.

2.12 N-(2-(2, 4-dimethylphenylthio) phenyl)-2-phenylacetamide (6i)

^{1}H NMR of N-(2-(2, 4-dimethylphenylthio) phenyl)-2-phenylacetamide (6i)

^{1}H NMR (DMSO-d_6): δ=2.22 (s, CH_3), 2.27(s, CH_3), 3.67(s, CH_2), 6.96 (m, Ar-3H), 7.10 (t, J=7.0 Hz, Ar-H), 7.14 (s, Ar-H), 7.28-7.22 (m, Ar-6H), 7.61 (d, J=7.0 Hz, Ar-H) and 9.47(s, NH) ppm.

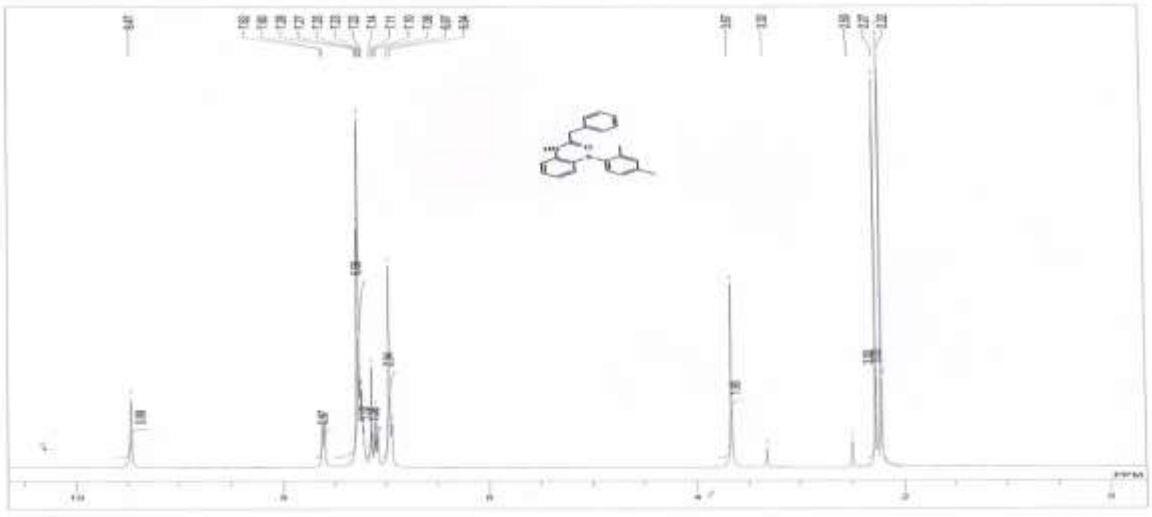

^{13}C NMR of N-(2-(2, 4-dimethylphenylthio) phenyl)-2-phenylacetamide (6i)

^{13}C NMR (DMSO-d_6): δ= 20.09, 20.75, 125.25, 126.21, 126.83, 127.78, 127.89, 128.54, 128.86, 129.26, 129.38, 131.13, 131.74, 131.96, 135.72, 136.93, 137.88, 139.08 and 169.63 ppm.

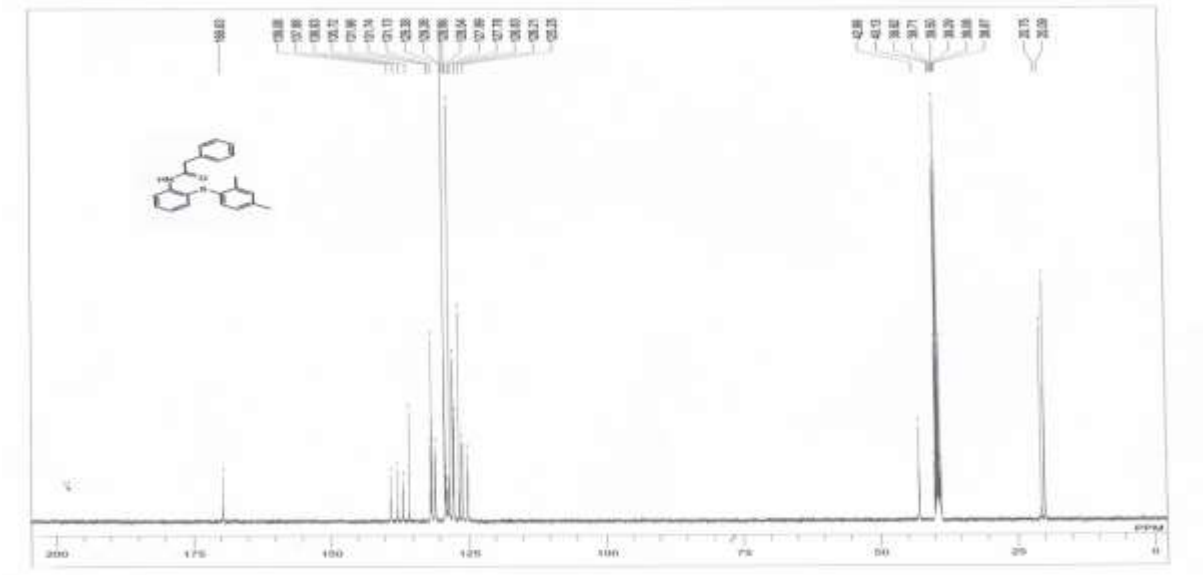

MS(EI) calculated for $C_{22}H_{21}NOS$ $[M+H]^+$: 348.1; found 348.1.

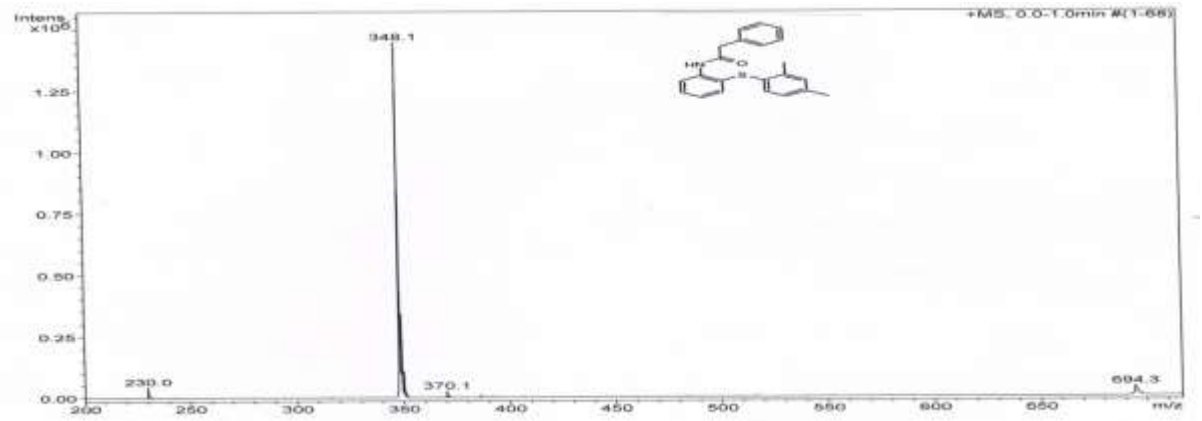

2.13 (2-(2, 4-dimethylphenylthio) phenylcarbamoyl) (phenyl) methyl acetate (6j)

^{1}H NMR of (2-(2, 4-dimethylphenylthio) phenylcarbamoyl) (phenyl) methyl acetate (6j)

^{1}H NMR (DMSO-d_6): δ=2.06 (s, CH_3), 2.29 (s, CH_3), 2.39(s, CH_3), 6.12 (s, CH), 6.53 (d, J=8.0 Hz, Ar-H), 6.83 (d, J=8.0 Hz, Ar-H), 7.04 (s, Ar-H), 7.12(m, Ar-H), 7.28 (m, Ar-6H), 7.39-7.44 (m, Ar-H), 7.48 (m, Ar-H), 8.49 (d, J=8.0 Hz, Ar-H), and 9.09 (s, -NH) ppm.

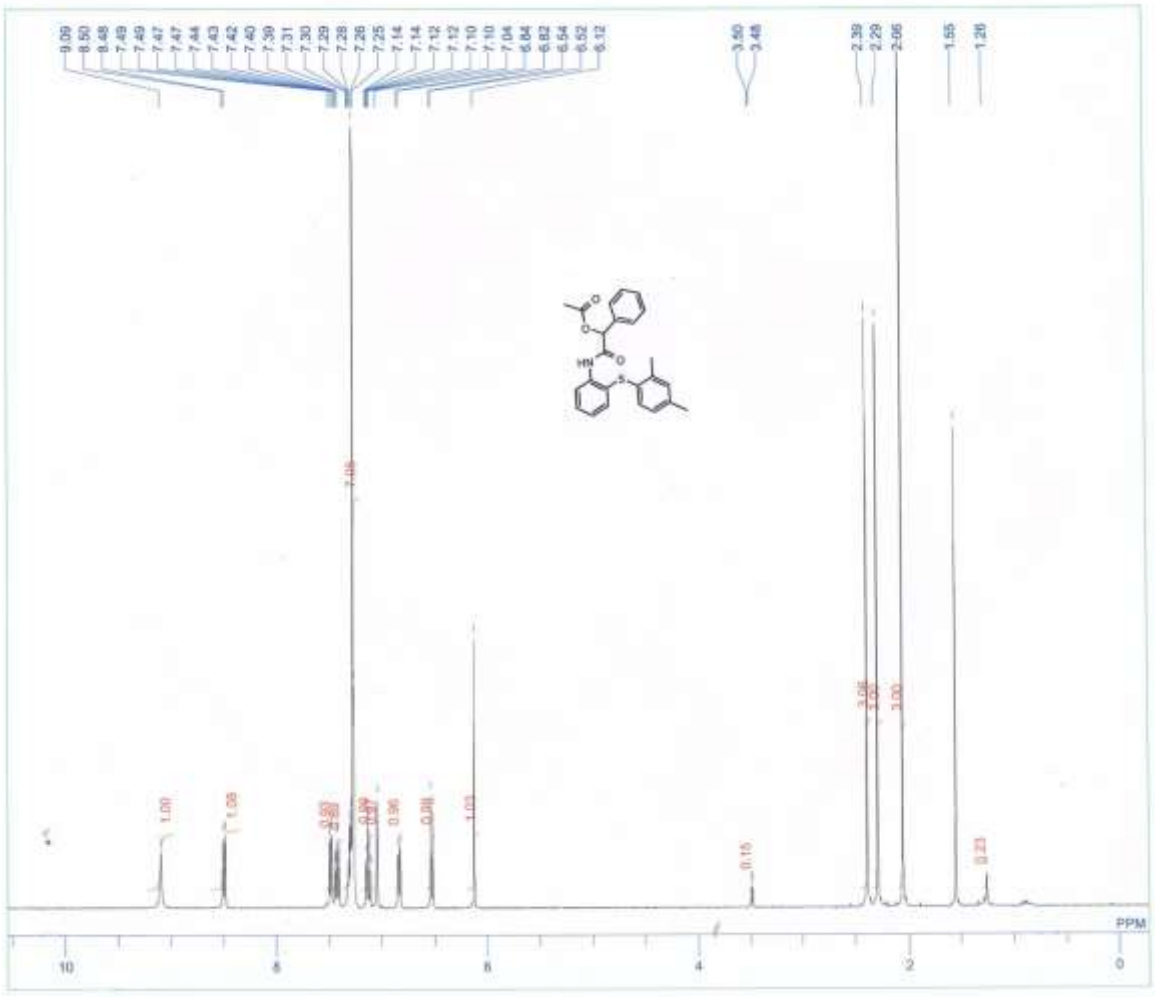

^{13}C NMR of (2-(2, 4-dimethylphenylthio) phenylcarbamoyl) (phenyl) methyl acetate (6j)

^{13}C NMR (DMSO-d_6): δ= 20.01, 20.59, 20.79, 75.81, 120.43, 125.0, 126.66, 127.26, 127.80, 128.70, 128.97, 130.59, 130.65, 131.39, 135.05, 135.52, 135.95, 136.14, 138.91, 166.37 and 168.72 ppm.

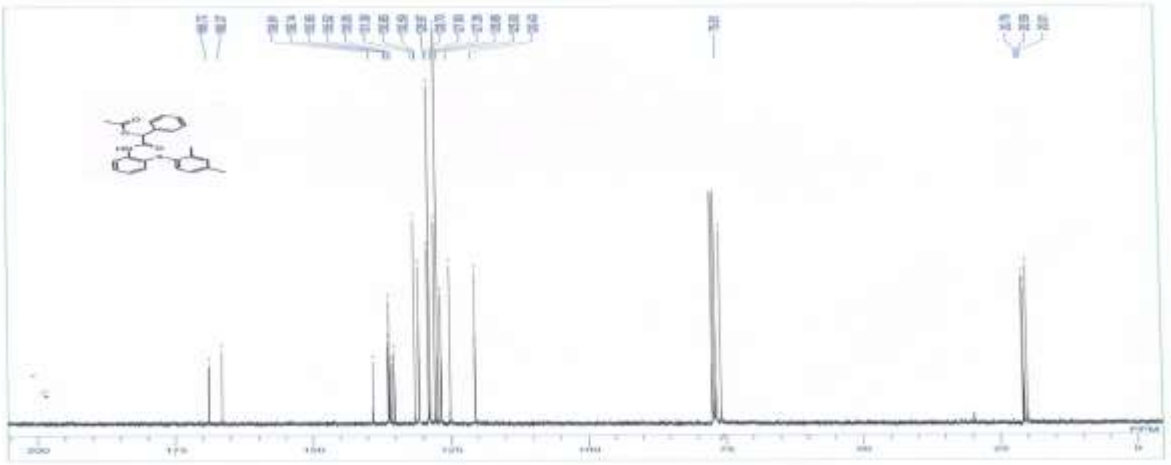

MS(EI) calculated for $C_{24}H_{23}NO_3S$ $[M+H]^+$: 406.1; found 406.1.

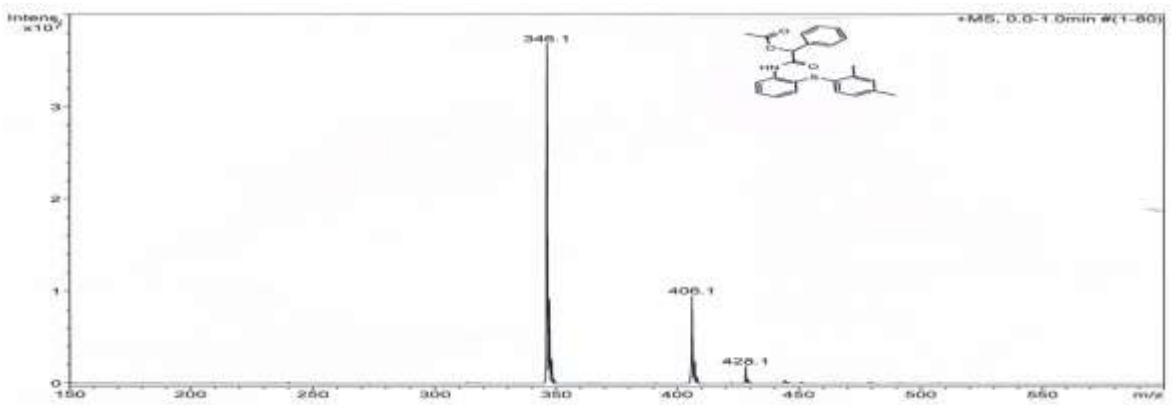

2.14 N-(2-(2, 4-dimethylphenylthio) phenyl)-5-methylpyrazine-2-carboxamide (6k)

*1*H NMR of N-(2-(2, 4-dimethylphenylthio) phenyl)-5-methylpyrazine-2-carboxamide (6k)

^{1}H NMR (DMSO-d_6): δ=2.22 (s, CH_3), 2.46(s, CH_3), 2.66 (s, CH_3), 6.82 (m, Ar-2H), 6.99 (s, Ar-H), 7.11-7.15 (m, Ar-H), 7.46 (m, Ar-2H), 8.39 (s, Ar-H), 8.63 (d, J=8.0 Hz, Ar-H), 9.30 (s, Ar-H) and 10.65 (s, -NH) ppm.

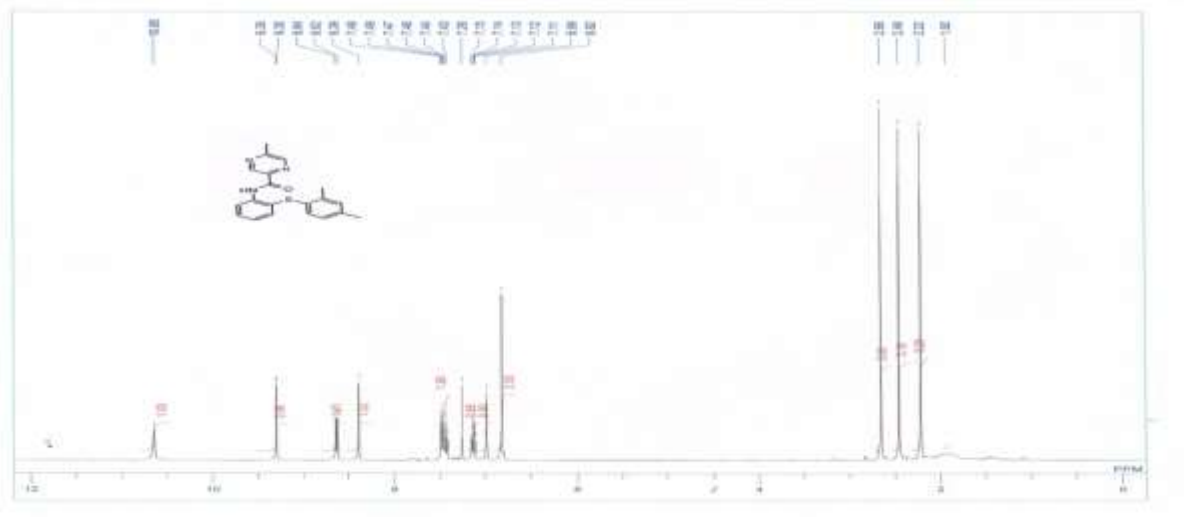

^{13}C NMR of N-(2-(2, 4-dimethylphenylthio) phenyl)-5-methylpyrazine-2-carboxamide (6k)

^{13}C NMR (DMSO-d_6): δ= 20.27, 20.77, 21.80, 120.68, 122.80, 124.73, 127.48, 128.96, 129.85, 130.66, 131.17, 135.32, 136.60, 137.21, 138.55, 141.88, 142.14, 143.41, 157.22, and 161.10 ppm.

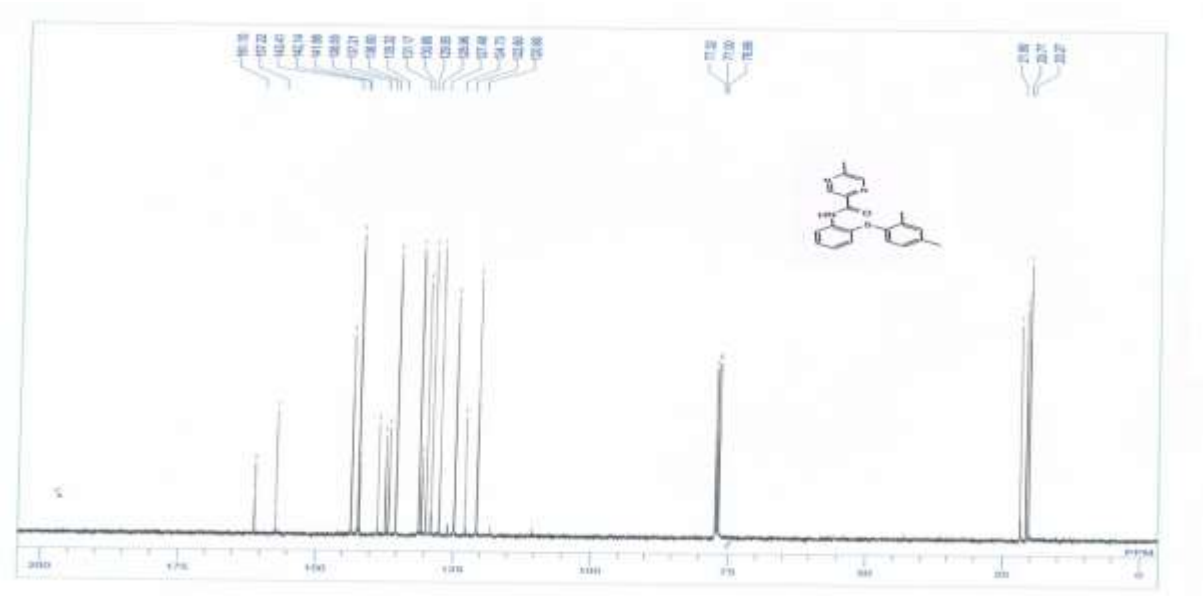

MS(EI) calculated for $C_{20}H_{19}N_3OS$ $[M+H]^+$: 350.1; found 349.9.

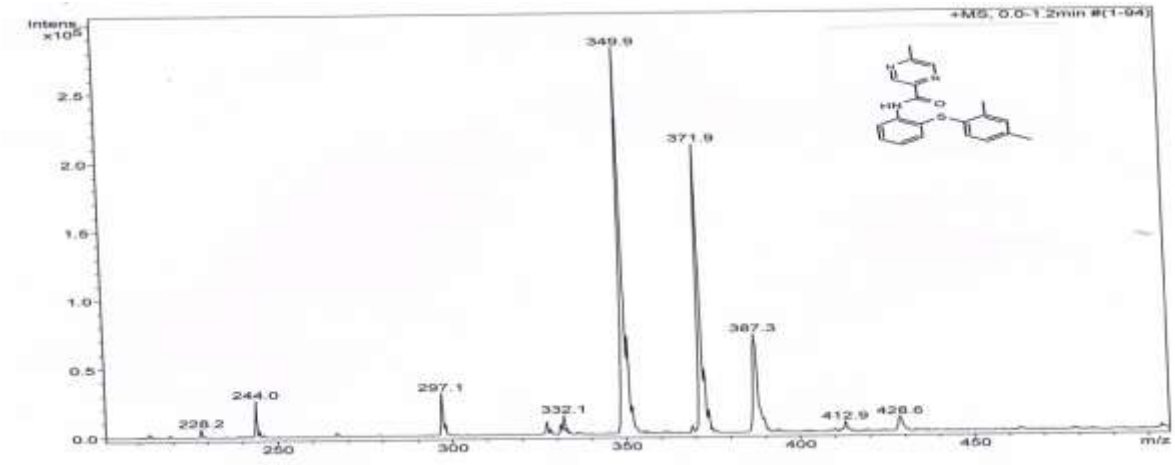

2.15 N-(2-(2, 4-dimethylphenylthio) phenyl) furan-2-carboxamide (6l)

*1*H NMR of N-(2-(2, 4-dimethylphenylthio) phenyl) furan-2-carboxamide (6l)

^{1}H NMR (DMSO-d_6): δ=2.25 (s, CH_3), 2.28(s, CH_3), 6.67 (s, Ar-H), 6.96 (s, Ar-H), 7.03 (m, Ar-2H), 7.08(d, J=8.0 Hz, Ar-H), 7.15 (t, J=7.0 Hz, Ar-H), 7.29 (m, Ar-2H), 7.71 (t, J=8.0 Hz, Ar-H), 7.88 (s, Ar-H) and 9.75(s, -NH) ppm.

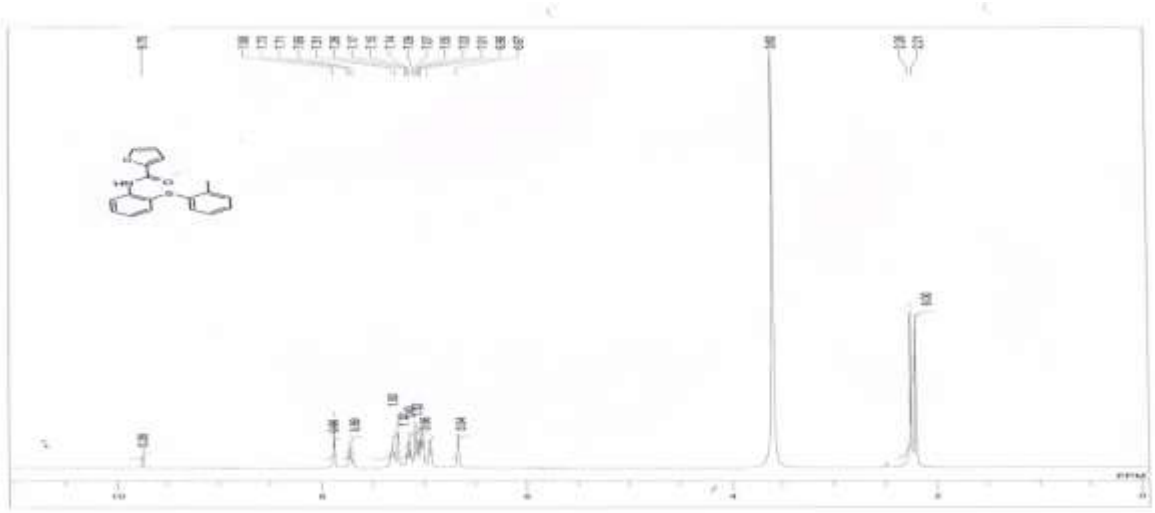

^{13}C NMR of N-(2-(2, 4-dimethylphenylthio) phenyl) furan-2-carboxamide (6l)

^{13}C NMR (DMSO-d_6): δ= 19.92, 20.48, 112.28, 114.94, 125.21, 126.27, 127.72, 128.99, 129.87, 131.01, 131.46, 132.24, 136.14, 137.77, 139.12, 145.74, 147.14, and 156.0 ppm.

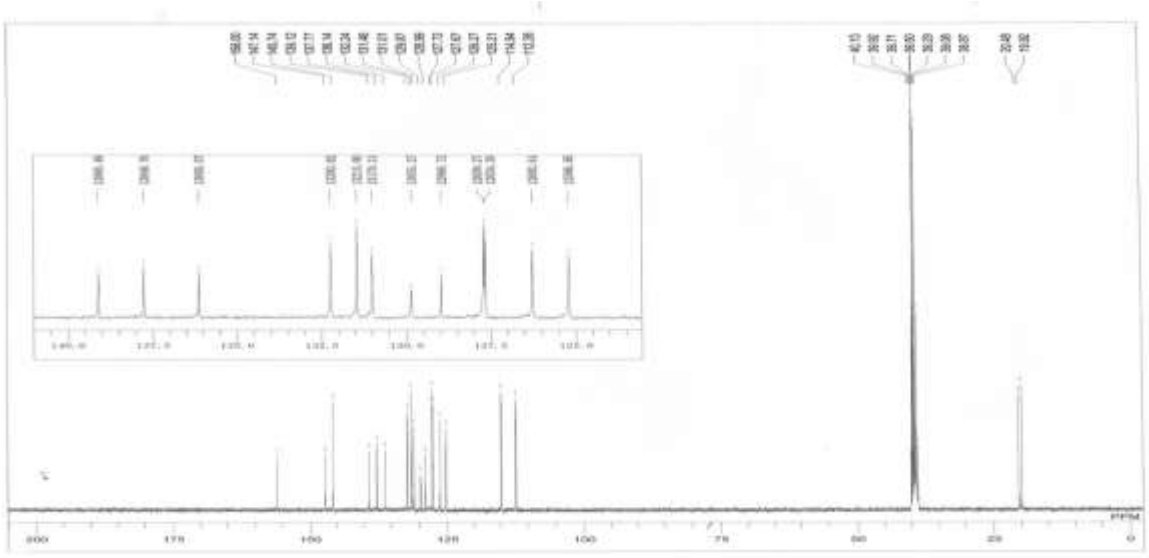

MS(EI) calculated for $C_{18}H_{15}NO_2S$ $[M+H]^+$: 324.1; found 324.3.

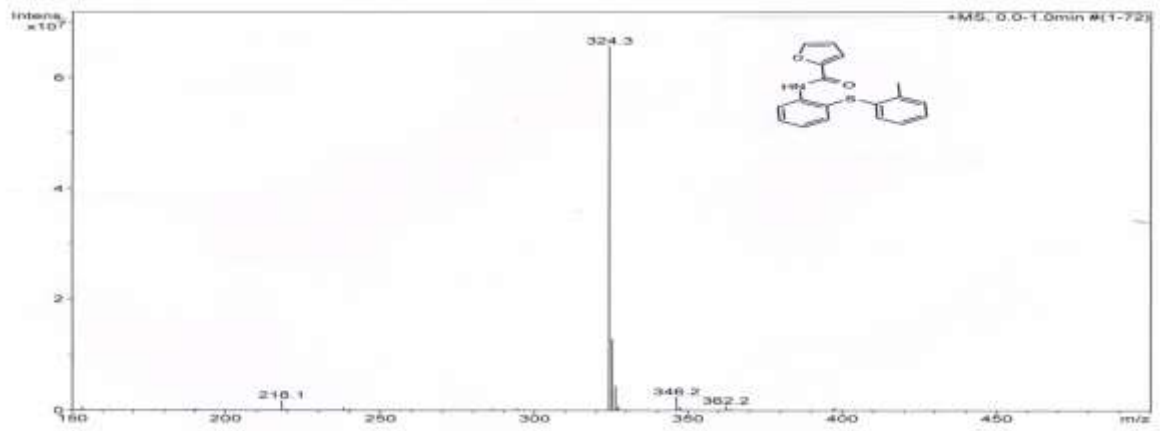

2.16 2-(2-(2, 4-dimethylphenylthio) phenylcarbamoyl) benzoic acid (6m)

*1*H NMR of 2-(2-(2, 4-dimethylphenylthio) phenylcarbamoyl) benzoic acid (6m)

^{1}H NMR (DMSO-d_6): δ=2.24 (s, CH_3), 2.29(s, CH_3), 6.88 (d, J=7.0 Hz, Ar-H), 7.03 (d, J=7.0 Hz, Ar-H), 7.15 (m, Ar-3H), 7.28(t, J=6.0 Hz, Ar-H), 7.42 (d, J=6.0 Hz, Ar-H) 7.56-7.64 (m, Ar-3H), 7.86 (d, J=7.0 Hz, Ar-H), 9.86 (s, -NH) and 13.06(s, -COOH) ppm.

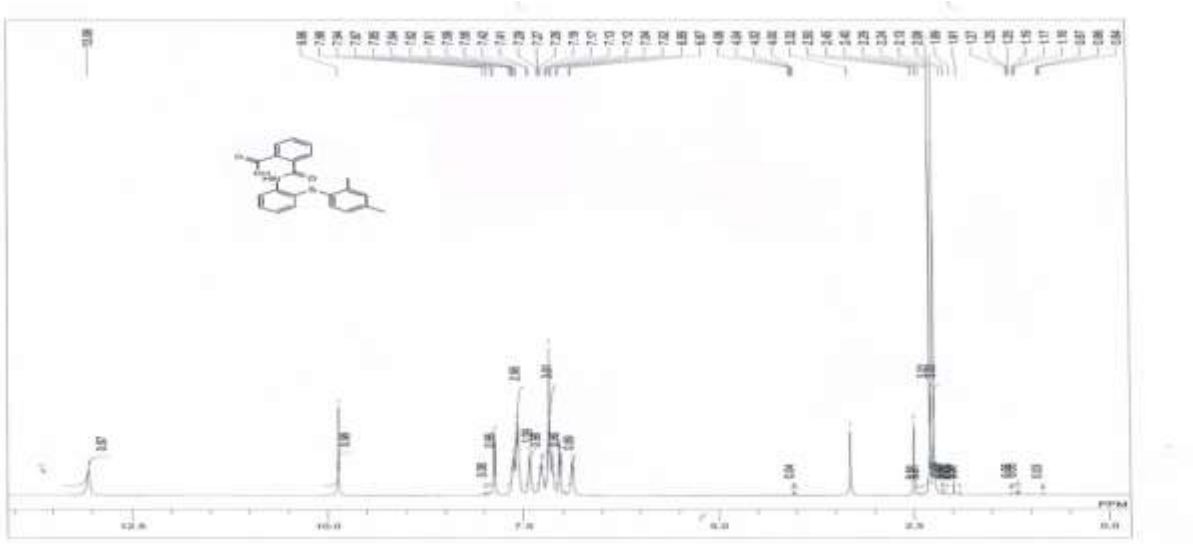

^{13}C NMR of 2-(2-(2, 4-dimethylphenylthio) phenylcarbamoyl) benzoic acid (6m)

^{13}C NMR (DMSO-d_6): δ= 20.10, 20.80, 115.3, 118.91, 125.25, 126.21, 126.83, 127.8, 128.7, 128.86, 129.26, 129.38, 131.13, 131.74, 131.96, 135.72, 136.93, 137.88, 139.08, 167.46 and 169.88 ppm.

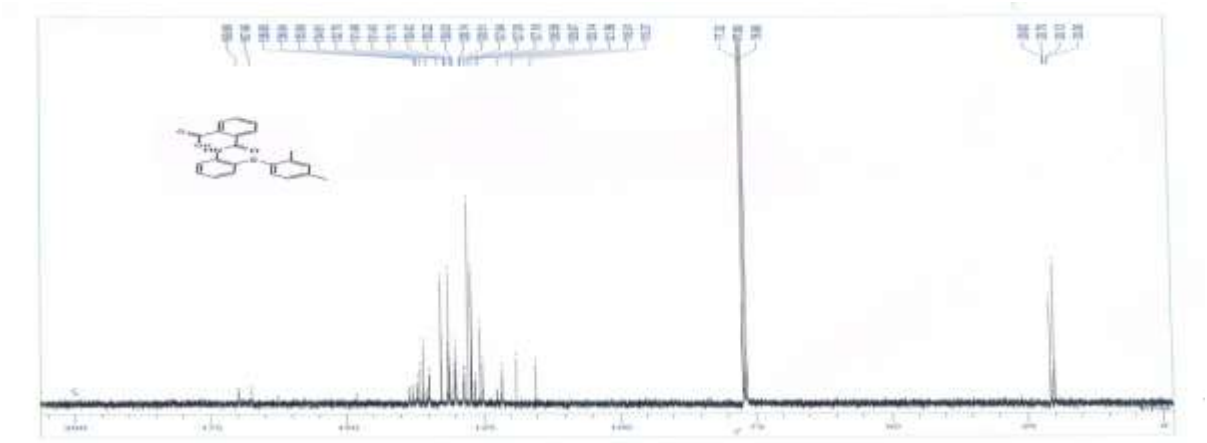

MS(EI) calculated for $C_{10}H_{17}N_3O_3$ $[M-H]^+$: 226.13; found 226.0.**N-(2-(2,4-2.17**

dimethylphenylthio)phenyl)-3-methylisoxazole-4-carboxamide (6n)

*1*H NMR of N-(2-(2, 4-dimethylphenylthio) phenyl)-3-methylisoxazole-4-carboxamide (6n)

^{1}H NMR (DMSO-d_6): δ=2.22 (s, CH_3), 2.27(s, CH_3), 2.65(s, CH_3), 6.87 (d, J=7.0 Hz, Ar-H), 7.01 (d, J=7.0 Hz, Ar-H), 7.14 (s, Ar-H), 7.16-7.19 (m, Ar-2H), 7.26 (t, J=6.0 Hz, Ar-H), 7.42 (d, J=6.0 Hz, Ar-H), 8.99 (s, Ar-H) and 9.87(s, -NH) ppm.

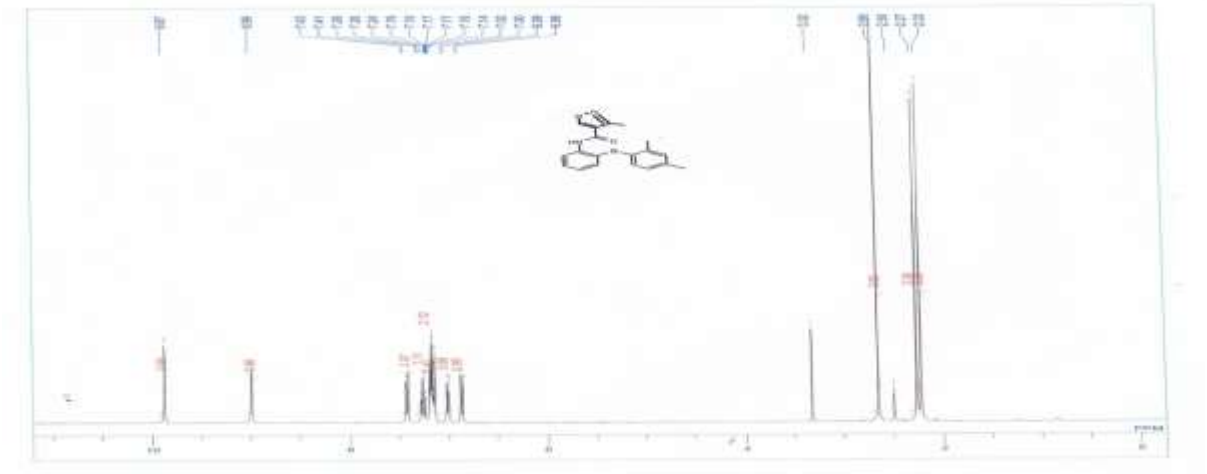

^{13}C NMR of N-(2-(2, 4-dimethylphenylthio) phenyl)-3-methylisoxazole-4-carboxamide (6n)

^{13}C NMR (DMSO-d_6): δ= 12.02, 20.0, 20.55, 111.53, 126.60, 127.07, 127.61, 127.74, 128.46, 129.12, 131.53, 133.24, 133.70, 135.16, 138.28, 140.06, 149.01, 159.37and 172.60 ppm.

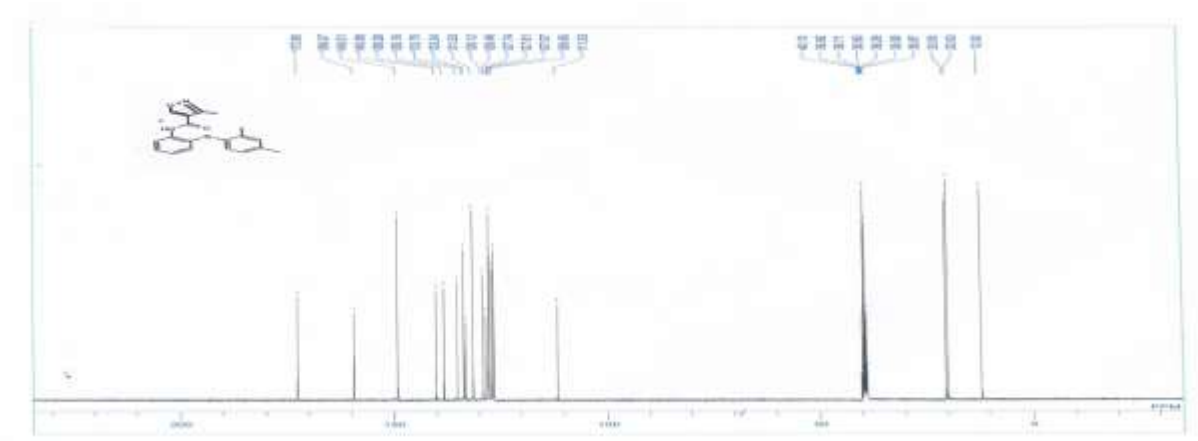

MS(EI) calculated for $C_{19}H_{18}N_2O_2S$ $[M+H]^+$: 339.1; found 339.0.

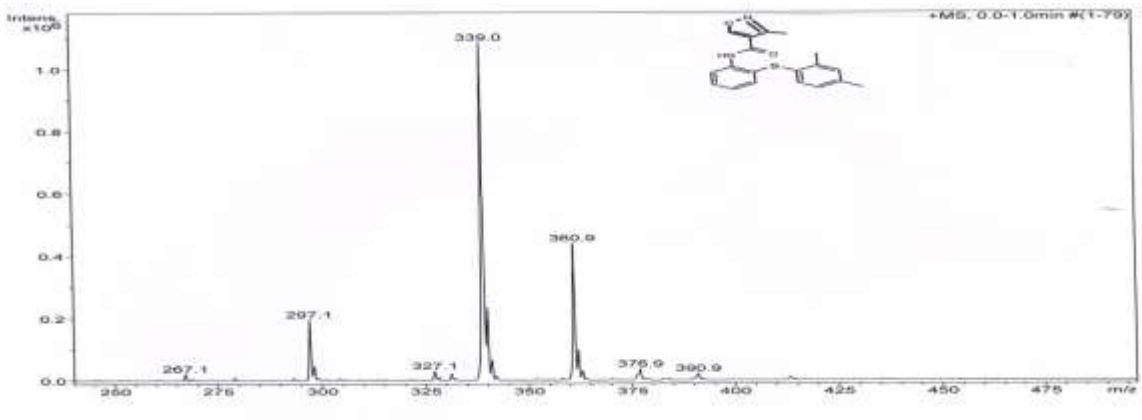

2.18 N-(2-(2, 4-dimethylphenylthio) phenyl)-5-chlorothiophene-2-carboxamide (6o)

*1*H NMR of N-(2-(2, 4-dimethylphenylthio) phenyl)-5-chlorothiophene-2-carboxamide (6o)

^{1}H NMR (DMSO-d_6): δ=2.22 (s, CH_3), 2.26(s, CH_3), 6.85 (d, J=7.0Hz, Ar-H), 7.01 (s, Ar-H), 7.14 (d, J=7.0 Hz, Ar-H), 7.19 (m, Ar-2H), 7.25 (m, Ar-2H), 7.41 (d, J=8.0 Hz, Ar-H), 7.86 (d, J= 4.0Hz, Ar-H) and 10.20(s, -NH) ppm.

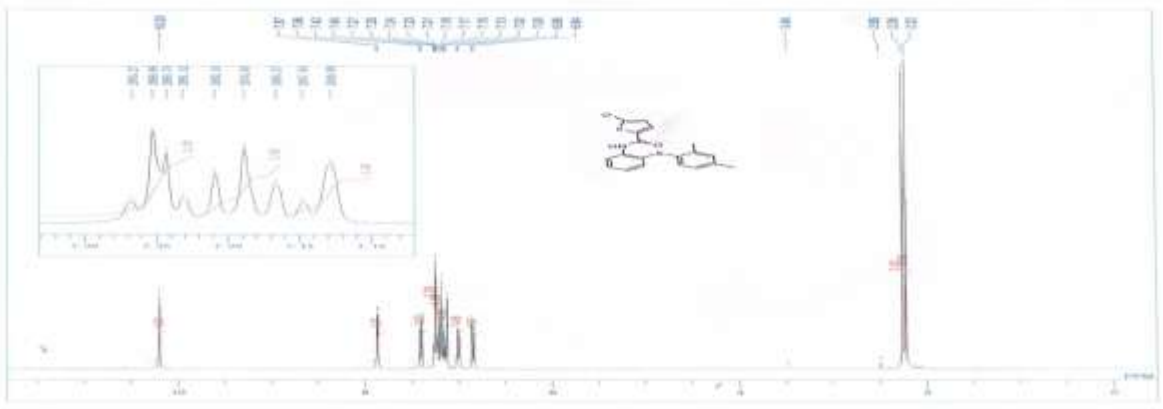

^{13}C NMR of N-(2-(2,4-dimethylphenylthio)phenyl)-5-chlorothiophene-2-carboxamide (6o)

^{13}C NMR (DMSO-d_6): δ= 20.03, 20.58, 126.54, 127.24, 127.74, 127.78, 128.21, 128.33, 128.87, 129.14, 131.56, 133.78, 133.85, 133.98, 134.97, 138.42, 140.24, and 159.07ppm.

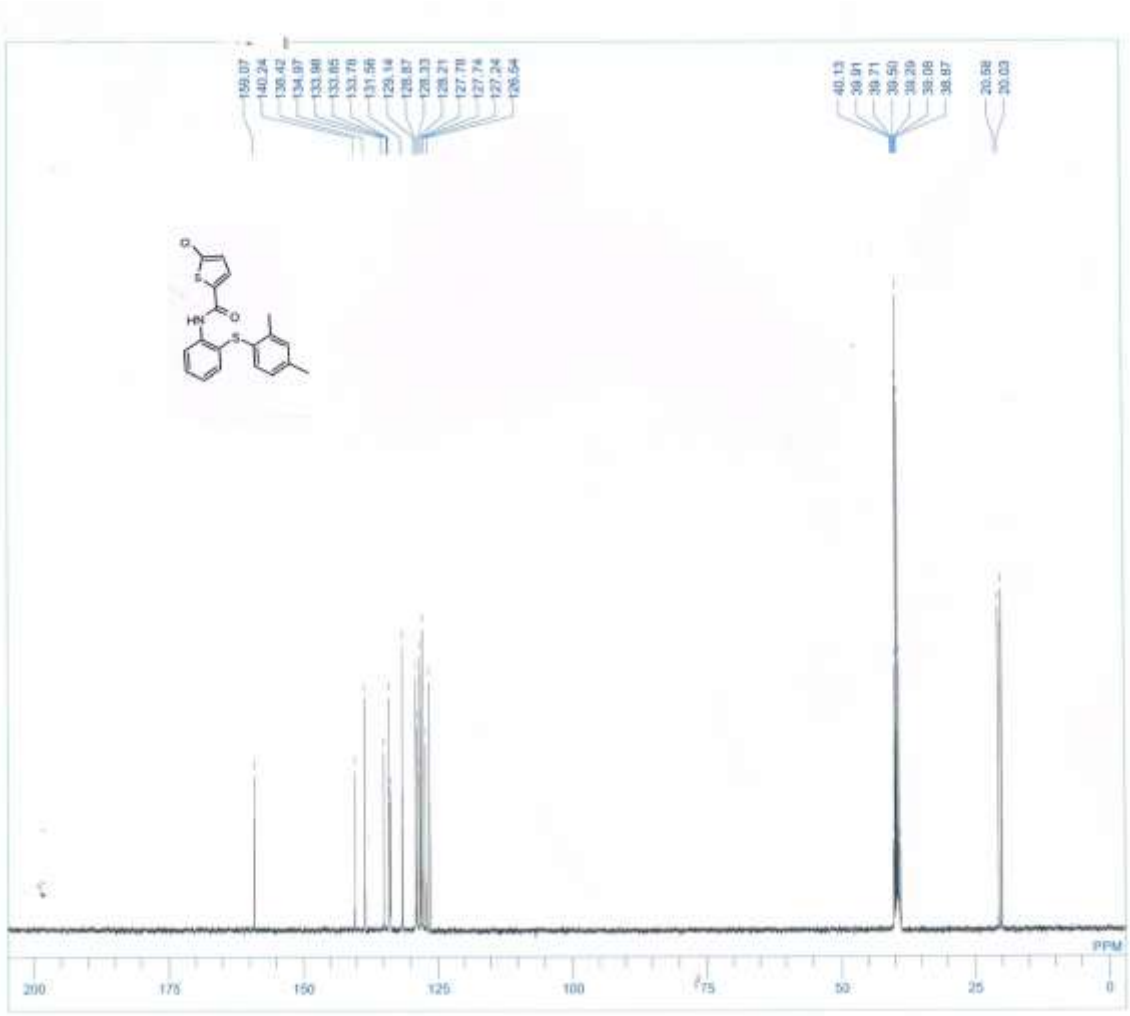

MS(EI) calculated for $C_{19}H_{16}ClNOS_2[M]^+$: 373.8; found 373.6.

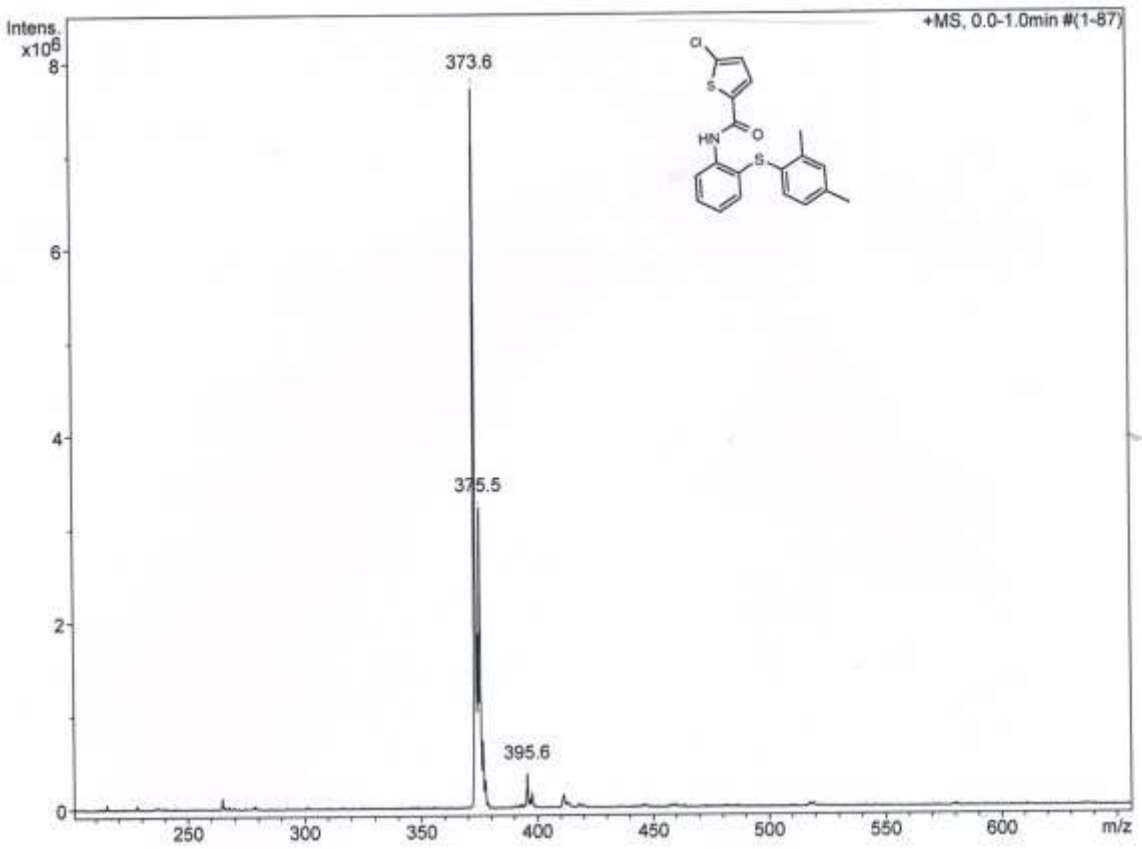
+MS, 0.0-1.0min #(1-87)
Intens.
x10^6
8
6
4
2
0
373.6
375.5
395.6
250
300
350
400
450
500
550
600
m/z
Cl
S
HN
O
S